

Optimum and Adaptive Complex-Valued Bilinear Filters

Bernhard Plaimer¹, Matthias Wagner¹, Oliver Lang¹, and Mario Huemer¹

¹Institute of Signal Processing, Johannes Kepler University, Linz, Austria

Abstract

The identification of nonlinear systems is a frequent task in digital signal processing. Such nonlinear systems may be grouped into many sub-classes, whereby numerous nonlinear real-world systems can be approximated as bilinear (BL) models. Therefore, various optimum and adaptive BL filters have been introduced in recent years. Further, in many applications such as communications and radar, complex-valued (CV) BL systems in combination with CV signals may occur.

Hence, in this work, we investigate the extension of real-valued (RV) BL filters to CV BL filters. First, we derive CV BL filters by applying two or four RV BL filters, and compare them with respect to their computational complexity and performance. Second, we introduce novel fully CV BL filters, such as the CV BL Wiener filter (WF), the CV BL least squares (LS) filter, the CV BL least mean squares (LMS) filter, the CV BL normalized LMS (NLMS) filter, and the CV BL recursive least squares (RLS) filter. Finally, these filters are applied to identify multiple-input-single-output (MISO) systems and Hammerstein models.

Index Terms

Adaptive algorithm, bilinear filter, complex-valued, system identification.

I. INTRODUCTION

IN many real-world applications, linear models provide sufficient descriptions of the input-output-relations of unknown systems. Hence, many linear optimum and adaptive filters, such as the the WF, the LS filter, the LMS filter, the NLMS filter, or the RLS filter are well established in the signal processing literature [1]–[3]. However, many applications exhibit distinct nonlinear behavior, which leads to nonlinear models. For the identification of nonlinear systems, Volterra filters [2], [4], neural networks (NNs) [5], spline adaptive filters (SAFs) [6] and many more have been introduced.

Since a number of nonlinear systems can be approximated by BL systems, quite some research on BL systems has been conducted [7]–[25]. Note that the BL term can be defined in two different ways. First, in [7]–[12] it appears with respect to the multiplication of input and output signals of systems. Second, in [13]–[25] the BL term is defined concerning the multiplication of system's coefficients. In recent years, the latter definition has been used to derive many BL optimum and adaptive filters, such as the BL WF [13], the BL LS filter [14], the BL LMS filter [15], [16], the BL NLMS filter [17], and the BL RLS filter [18]–[21]. As summarized in Table I, the current state of the art covers solely RV BL filters. In many applications, e.g., in communications, also CV BL systems in combination with CV signals may occur [26], [27].

Hence, in this work, we extend the aforementioned RV BL filters to the complex domain. Note that two main approaches can be distinguished for deriving CV filters. The first one is the split-CV approach, where two or four RV filters are used to approximate the real- and the imaginary-part of a desired signal, as presented for linear filters in [28]–[30]. In Table I and the remainder of this work, these methods are referred to as $2\mathbb{R}$ and $4\mathbb{R}$ filter structures, respectively. Obviously, the $4\mathbb{R}$ filter structure may deal with signals, which show a correlation between the real- and the imaginary parts as opposed to the $2\mathbb{R}$ filter structure. The second approach to derive CV filters is to use actual CV filter coefficients, which will be referred to as fully CV filter structure in the sequel. These fully CV filters may show a number of advantages [31], [32]:

- As the $4\mathbb{R}$ filters they may also cope with a correlation between the real- and the imaginary parts of the signals.
- They might be more natural.
- They can be implemented with lower complexity.
- They typically allow for a more compact mathematical representation.
- In contrast to CV linear filters, not every fully CV BL system can be represented by a $4\mathbb{R}$ BL filter.

In this work, after a brief introduction and analysis of the $2\mathbb{R}$ and $4\mathbb{R}$ BL filter structures, we introduce several novel fully CV BL filters, such as the CV BL WF, the CV BL LS filter, the CV BL LMS filter, the CV BL NLMS filter, and the CV BL RLS filter. For the sake of completeness, the update equations for mixed CV-RV BL filters, where one of the two coefficient vectors is assumed to be RV, are also derived. A comprehensive overview of already existing and in this paper derived optimum and adaptive BL filters can be seen in Table I. In addition to the derivations of these filters, convergence analyses are carried out for both the CV BL WF and the CV BL LMS-based filters. In this work, we additionally present representative applications of the proposed filters in the form of MISO systems as in [13]–[24] and Hammerstein models [33], [34].

The rest of this paper is structured as follows. In Section II, the CV BL model is introduced. $2\mathbb{R}$ BL filters, $4\mathbb{R}$ BL filters, fully CV BL filters, and mixed CV-RV BL filters are derived in Section III. Simulation results are presented in Section IV,

TABLE I
OVERVIEW OF OPTIMUM AND ADAPTIVE BL FILTERS

Filter type	RV BL filter	$2\mathbb{R}$	CV BL filter structures	Fully CV	Mixed CV-RV
WF	[13]	analogously to Section III-A	analogously to Section III-B	Section III-C	Section III-H
LS	[14]	analogously to Section III-A	analogously to Section III-B	Section III-D	Section III-H
LMS	[15], [16]	Section III-A	Section III-B	Section III-E	Section III-H
NLMS	[17]	analogously to Section III-A	analogously to Section III-B	Section III-F	Appendix V-A
RLS	[18]–[21]	analogously to Section III-A	analogously to Section III-B	Section III-G	Section III-H

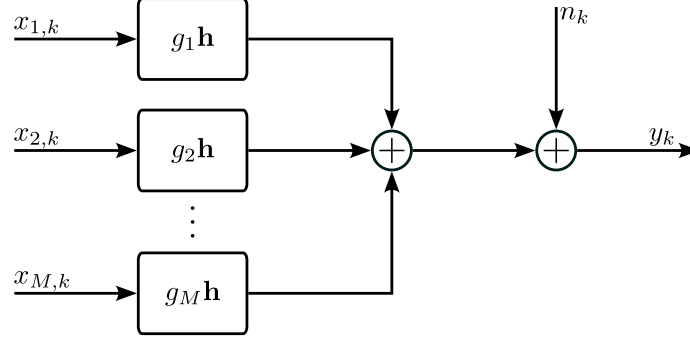


Fig. 1. Block diagram of a MISO system.

and finally, Section V concludes this work.

Notation and Definitions:

Lower and upper case boldface letters denote vectors and matrices, respectively. Underlined vectors indicate the CV augmentations of vectors, e.g., $\underline{\mathbf{x}} = [\mathbf{x}^T \mathbf{x}^H]^T$, where $(\cdot)^T$ indicates the transposition, and $(\cdot)^H$ indicates the complex conjugate transposition. Further, $(\cdot)^*$ indicates the complex conjugate, and $\text{tr}[\cdot]$ indicates the trace of a matrix. To represent an identity matrix $\mathbf{I}^{m \times m}$ is used, while the zero matrix is denoted by $\mathbf{0}^{m \times n}$. The superscripts indicate the dimensions. The expectation operator is denoted by $\mathbb{E}[\cdot]$, and the real and imaginary parts of a variable are indicated by $\text{Re}[\cdot]$ and $\text{Im}[\cdot]$, respectively. Further, the imaginary unit is represented by j . The vectorization operator is defined as

$$\mathbf{a} = \text{vec}[\mathbf{A}] = \text{vec}[\mathbf{a}_1 \quad \cdots \quad \mathbf{a}_M] = \begin{bmatrix} \mathbf{a}_1 \\ \vdots \\ \mathbf{a}_M \end{bmatrix} \in \mathbb{C}^{LM}, \quad (1)$$

where $\mathbf{a}_m \in \mathbb{C}^L$ denotes the m th column of $\mathbf{A} \in \mathbb{C}^{L \times M}$. The operator $\text{mat}_M[\cdot]$ is the inverse of the vectorization operator as described in (1) and is defined as

$$\mathbf{A} = \text{mat}_M[\mathbf{a}] = \text{mat}_M \begin{bmatrix} \mathbf{a}_1 \\ \vdots \\ \mathbf{a}_M \end{bmatrix} = [\mathbf{a}_1 \quad \cdots \quad \mathbf{a}_M], \quad (2)$$

where the vector \mathbf{a} is split into M sub-vectors \mathbf{a}_m of length L . The operator \otimes is used for the Kronecker product.

II. COMPLEX-VALUED BILINEAR MODEL

In this work, a CV BL system is represented by the input-output relation

$$y_k = \mathbf{h}^H \mathbf{X}_k \mathbf{g} + n_k, \quad (3)$$

with $y_k \in \mathbb{C}$ as the output signal, $\mathbf{X}_k \in \mathbb{C}^{L \times M}$ as the input signal matrix, and $n_k \in \mathbb{C}$ as CV noise at a time-instance k . The matrix \mathbf{X}_k depends on the values of the input signal x_k , and its structure heavily depends on the application at hand. As an example, the input-output relation of a MISO system, as can be seen in Figure 1, may be written in the form of (3). With M input signals $x_{m,k}$ in combination with M linear channels $g_m \mathbf{h} \in \mathbb{C}^L$, for $m = 1, \dots, M$, the input signal matrix follows to

$$\mathbf{X}_k = [\mathbf{x}_{1,k} \quad \mathbf{x}_{2,k} \quad \cdots \quad \mathbf{x}_{M,k}], \quad (4)$$

where the m th column $\mathbf{x}_{m,k}$ consists of the past L input samples of the input signal $x_{m,k}$. The scalar $g_m \in \mathbb{C}$ is the m th entry of $\mathbf{g} \in \mathbb{C}^M$, and it may represent an amplitude and phase difference among the M different channels.

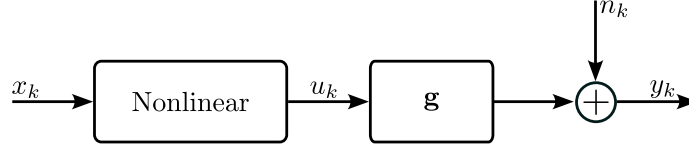


Fig. 2. Block diagram of a Hammerstein system.

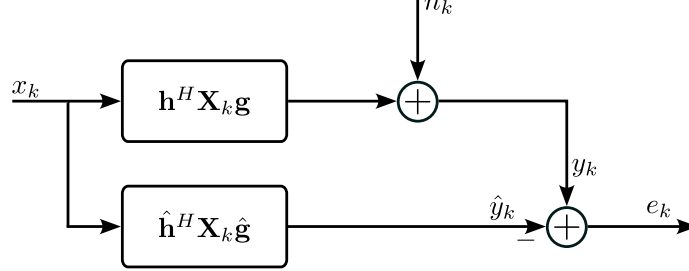


Fig. 3. Block diagram of a system identification task using optimum or adaptive filters.

In a second example, consider a Hammerstein system, as can be seen in Figure 2. Assuming the nonlinearity is memory-free and linear in the parameters as

$$u_k = \sum_{l=1}^L h_l^* \varphi_l(x_k), \quad (5)$$

with nonlinear functions $\varphi_l(x_k)$ and parameters h_l , the input-output relation of this Hammerstein system again can be written in the form of (3). The corresponding input signal matrix results in

$$\mathbf{X}_k = \begin{bmatrix} \varphi_1(x_k) & \cdots & \varphi_1(x_{k-M+1}) \\ \vdots & \ddots & \vdots \\ \varphi_L(x_k) & \cdots & \varphi_L(x_{k-M+1}) \end{bmatrix}. \quad (6)$$

In both applications, the vectors $\mathbf{h} \in \mathbb{C}^L$ and $\mathbf{g} \in \mathbb{C}^M$ can be interpreted as coefficient vectors.

By analyzing (3), it is easy to see that every BL model can be rewritten as a linear model as

$$y_k = \mathbf{f}^T \tilde{\mathbf{x}}_k + n_k, \quad (7)$$

where we denote $\mathbf{f} = \mathbf{g} \otimes \mathbf{h}^* \in \mathbb{C}^{LM}$ as the equivalent linear coefficient vector and $\tilde{\mathbf{x}}_k = \text{vec}[\mathbf{X}_k] \in \mathbb{C}^{LM}$ as the equivalent input vector.

Using optimum or adaptive filters, with their key structure illustrated in Figure 3, the goal is to find filter parameters $\hat{\mathbf{h}} \in \mathbb{C}^L$ and $\hat{\mathbf{g}} \in \mathbb{C}^M$ or $\hat{\mathbf{f}} \in \mathbb{C}^{LM}$ that minimize a costfunction based on the error signal e_k . While a bilinear system has $L + M$ unknown parameters, finding $\hat{\mathbf{f}}_k$ directly requires LM parameters to be found. Note that it is only possible to estimate \mathbf{h} and \mathbf{g} up to a CV constant $\nu \in \mathbb{C}$, since

$$\mathbf{h}^H \mathbf{X}_k \mathbf{g} = (\nu \mathbf{h})^H \mathbf{X}_k \mathbf{g} \frac{1}{\nu^*}, \quad (8)$$

while \mathbf{f} is unaffected by this scaling factor.

III. COMPLEX-VALUED BILINEAR FILTERS

In the following chapter, several CV BL filters are derived. To approximate the output of a system as in (3), we investigate four different methods. First, this can be achieved by using either $2\mathbb{R}$ or $4\mathbb{R}$ BL filter structures. Second, a fully CV BL filter structure is applied to estimate \mathbf{h} and \mathbf{g} . The fourth method is based on the equivalent linear system shown in (7), thus a CV linear filter may be used [31], [32], [35], [36]. However, this may result in slow convergence speeds because LM coefficients have to be estimated instead of $L + M$ in the BL case.

It should be noted that $2\mathbb{R}$ BL filters and $4\mathbb{R}$ BL filters may be interpreted as simple extensions from the vast literature on RV BL filters [13]–[24]. Thus, in this work only the derivations of the $2\mathbb{R}$ BL LMS filter and the $4\mathbb{R}$ BL LMS filter are shown. The derivations of further $2\mathbb{R}$ and $4\mathbb{R}$ optimum and adaptive BL filters can be carried out similarly.

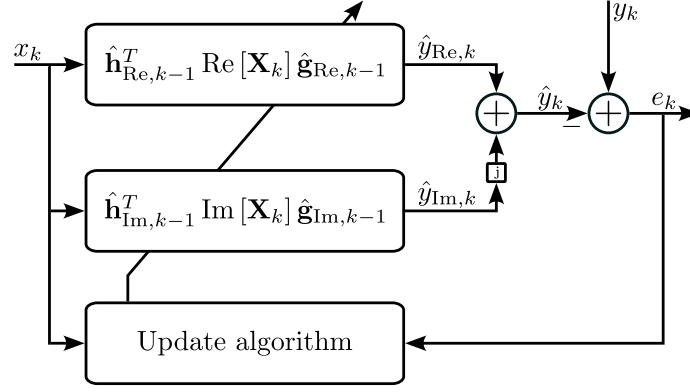


Fig. 4. Block diagram of a $2\mathbb{R}$ BL filter structure.

A. $2\mathbb{R}$ BL LMS filter

The output of a $2\mathbb{R}$ BL LMS filter, as can be seen in Figure 4, may be written as

$$\hat{y}_k = \hat{\mathbf{h}}_{\text{Re},k-1}^T \text{Re}[\mathbf{X}_k] \hat{\mathbf{g}}_{\text{Re},k-1} + j \hat{\mathbf{h}}_{\text{Im},k-1}^T \text{Im}[\mathbf{X}_k] \hat{\mathbf{g}}_{\text{Im},k-1} \quad (9)$$

$$= \hat{y}_{\text{Re},k} + j \hat{y}_{\text{Im},k}, \quad (10)$$

with $\hat{\mathbf{h}}_{\text{Re},k}, \hat{\mathbf{h}}_{\text{Im},k} \in \mathbb{R}^L$, and $\hat{\mathbf{g}}_{\text{Re},k}, \hat{\mathbf{g}}_{\text{Im},k} \in \mathbb{R}^M$. Note that (9) incorporates two RV BL LMS filters as discussed in [15]. With that, the error signal

$$e_k = y_k - \hat{y}_k \quad (11)$$

$$= \text{Re}[y_k] - \hat{y}_{\text{Re},k} + j(\text{Im}[y_k] - \hat{y}_{\text{Im},k}) \quad (12)$$

$$= e_{\text{Re},k} + j e_{\text{Im},k} \quad (13)$$

and the instantaneous squared error (ISE) as the cost function

$$J_k = e_k e_k^* \quad (14)$$

can be formulated. Utilizing this cost function, the gradient descent based update equations for the filter coefficients follow as

$$\hat{\mathbf{h}}_{\text{Re},k} = \hat{\mathbf{h}}_{\text{Re},k-1} - \mu_{\mathbf{h}_{\text{Re}}} \frac{\partial J_k}{\partial \hat{\mathbf{h}}_{\text{Re},k-1}}, \quad (15)$$

$$\hat{\mathbf{h}}_{\text{Im},k} = \hat{\mathbf{h}}_{\text{Im},k-1} - \mu_{\mathbf{h}_{\text{Im}}} \frac{\partial J_k}{\partial \hat{\mathbf{h}}_{\text{Im},k-1}} \quad (16)$$

and

$$\hat{\mathbf{g}}_{\text{Re},k} = \hat{\mathbf{g}}_{\text{Re},k-1} - \mu_{\mathbf{g}_{\text{Re}}} \frac{\partial J_k}{\partial \hat{\mathbf{g}}_{\text{Re},k-1}}, \quad (17)$$

$$\hat{\mathbf{g}}_{\text{Im},k} = \hat{\mathbf{g}}_{\text{Im},k-1} - \mu_{\mathbf{g}_{\text{Im}}} \frac{\partial J_k}{\partial \hat{\mathbf{g}}_{\text{Im},k-1}}, \quad (18)$$

where $\mu_{\mathbf{h}_{\text{Re}}}, \mu_{\mathbf{h}_{\text{Im}}}, \mu_{\mathbf{g}_{\text{Re}}}, \mu_{\mathbf{g}_{\text{Im}}} \in \mathbb{R}$ are the step-sizes. Inserting the gradients yields

$$\hat{\mathbf{h}}_{\text{Re},k} = \hat{\mathbf{h}}_{\text{Re},k-1} + \mu_{\mathbf{h}_{\text{Re}}} e_{\text{Re},k} \text{Re}[\mathbf{X}_k] \hat{\mathbf{g}}_{\text{Re},k-1}, \quad (19)$$

$$\hat{\mathbf{h}}_{\text{Im},k} = \hat{\mathbf{h}}_{\text{Im},k-1} + \mu_{\mathbf{h}_{\text{Im}}} e_{\text{Im},k} \text{Im}[\mathbf{X}_k] \hat{\mathbf{g}}_{\text{Im},k-1}. \quad (20)$$

Further, the update equations for $\hat{\mathbf{g}}_{\text{Re},k}$ and $\hat{\mathbf{g}}_{\text{Im},k}$ become

$$\hat{\mathbf{g}}_{\text{Re},k} = \hat{\mathbf{g}}_{\text{Re},k-1} + \mu_{\mathbf{g}_{\text{Re}}} e_{\text{Re},k} \text{Re}[\mathbf{X}_k^T] \hat{\mathbf{h}}_{\text{Re},k-1}, \quad (21)$$

$$\hat{\mathbf{g}}_{\text{Im},k} = \hat{\mathbf{g}}_{\text{Im},k-1} + \mu_{\mathbf{g}_{\text{Im}}} e_{\text{Im},k} \text{Im}[\mathbf{X}_k^T] \hat{\mathbf{h}}_{\text{Im},k-1}. \quad (22)$$

Computational complexity:

To compute (19) and (20), $2(LM + L + 1)$ RV scalar multiplications are necessary. Analogously, for (21) and (22), $2(LM + M + 1)$ RV scalar multiplications are needed. When calculating the error $e_{\text{Re},k}$, the first BL term in (9) can be evaluated in two different ways by either starting with $\text{Re}[\mathbf{X}_k] \hat{\mathbf{g}}_{\text{Re},k-1}$ or with $\hat{\mathbf{h}}_{\text{Re},k-1}^T \text{Re}[\mathbf{X}_k]$. Similarly, also $e_{\text{Im},k}$ can be

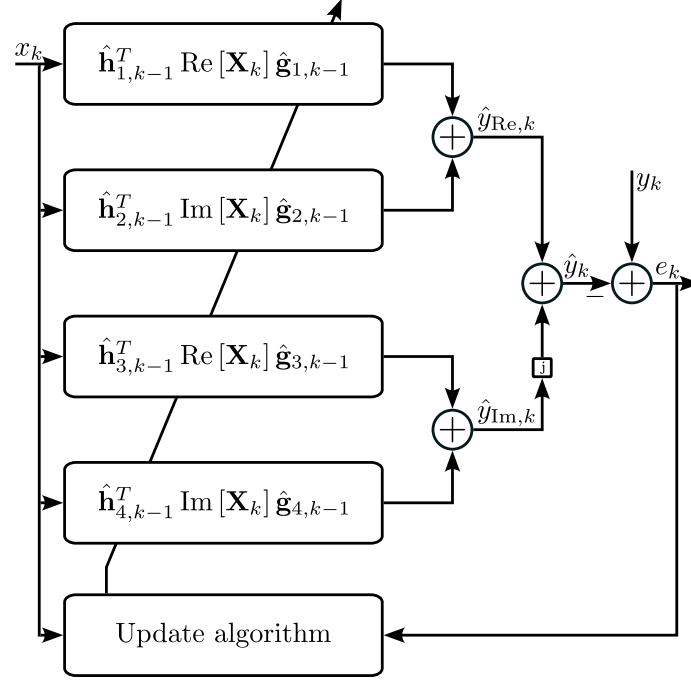


Fig. 5. Block diagram of a 4 \mathbb{R} BL filter structure.

calculated in two different ways. This yields $LM + L$ or $LM + M$ RV scalar multiplications, respectively. In total, this sums up to

$$N_{2\mathbb{R},1} = 6LM + 2L + 4M + 4 \quad (23)$$

or

$$N_{2\mathbb{R},2} = 6LM + 4L + 2M + 4 \quad (24)$$

RV scalar multiplications.

Remark:

To identify a system that introduces a correlation between the real- and the imaginary part of the output signal, it is well known from linear filters that this method may perform poorly [31], [32]. The utilization of 4 \mathbb{R} BL LMS filters may circumvents this problem as discussed in the following.

B. 4 \mathbb{R} BL LMS filter

When using four RV BL filters, as shown in Figure 5, the filtered output becomes

$$\hat{y}_k = \hat{\mathbf{h}}_{1,k-1}^T \text{Re}[\mathbf{X}_k] \hat{\mathbf{g}}_{1,k-1} + \hat{\mathbf{h}}_{2,k-1}^T \text{Im}[\mathbf{X}_k] \hat{\mathbf{g}}_{2,k-1} + j \left(\hat{\mathbf{h}}_{3,k-1}^T \text{Re}[\mathbf{X}_k] \hat{\mathbf{g}}_{3,k-1} + \hat{\mathbf{h}}_{4,k-1}^T \text{Im}[\mathbf{X}_k] \hat{\mathbf{g}}_{4,k-1} \right) \quad (25)$$

$$= \hat{y}_{\text{Re},k} + j\hat{y}_{\text{Im},k}, \quad (26)$$

with $\hat{\mathbf{h}}_{l,k} \in \mathbb{R}^L$ and $\hat{\mathbf{g}}_{l,k} \in \mathbb{R}^M$ where $l = 1, \dots, 4$. The same error signal and cost function as in (13) and (14) are used but with the estimated output (26). Again using the gradient descent technique with the step-sizes $\mu_{\mathbf{h}_i} \in \mathbb{R}$ and $\mu_{\mathbf{g}_i} \in \mathbb{R}$ the update equations become

$$\hat{\mathbf{h}}_{i,k} = \hat{\mathbf{h}}_{i,k-1} - \mu_{\mathbf{h}_i} \frac{\partial J_k}{\partial \hat{\mathbf{h}}_{i,k-1}}, \quad (27)$$

$$\hat{\mathbf{g}}_{i,k} = \hat{\mathbf{g}}_{i,k-1} - \mu_{\mathbf{g}_i} \frac{\partial J_k}{\partial \hat{\mathbf{g}}_{i,k-1}}, \quad (28)$$

for $i = 1, \dots, 4$. Evaluating the gradients yields

$$\hat{\mathbf{h}}_{1,k} = \hat{\mathbf{h}}_{1,k-1} + \mu_{\mathbf{h}_1} e_{\text{Re},k} \text{Re}[\mathbf{X}_k] \hat{\mathbf{g}}_{1,k-1}, \quad (29)$$

$$\hat{\mathbf{h}}_{2,k} = \hat{\mathbf{h}}_{2,k-1} + \mu_{\mathbf{h}_2} e_{\text{Re},k} \text{Im}[\mathbf{X}_k] \hat{\mathbf{g}}_{2,k-1}, \quad (30)$$

$$\hat{\mathbf{h}}_{3,k} = \hat{\mathbf{h}}_{3,k-1} + \mu_{\mathbf{h}_3} e_{\text{Im},k} \text{Re}[\mathbf{X}_k] \hat{\mathbf{g}}_{3,k-1}, \quad (31)$$

$$\hat{\mathbf{h}}_{4,k} = \hat{\mathbf{h}}_{4,k-1} + \mu_{\mathbf{h}_4} e_{\text{Im},k} \text{Im}[\mathbf{X}_k] \hat{\mathbf{g}}_{4,k-1}, \quad (32)$$

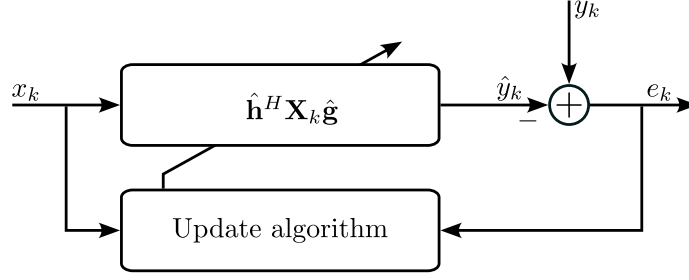


Fig. 6. Block diagram of a fully CV BL filter structure.

and

$$\hat{\mathbf{g}}_{1,k} = \hat{\mathbf{g}}_{1,k-1} + \mu_{\mathbf{g}_1} e_{\text{Re},k} \text{Re} [\mathbf{X}_k^T] \hat{\mathbf{h}}_{1,-1k}, \quad (33)$$

$$\hat{\mathbf{g}}_{2,k} = \hat{\mathbf{g}}_{2,k-1} + \mu_{\mathbf{g}_2} e_{\text{Re},k} \text{Im} [\mathbf{X}_k^T] \hat{\mathbf{h}}_{2,k-1}, \quad (34)$$

$$\hat{\mathbf{g}}_{3,k} = \hat{\mathbf{g}}_{3,k-1} + \mu_{\mathbf{g}_3} e_{\text{Im},k} \text{Re} [\mathbf{X}_k^T] \hat{\mathbf{h}}_{3,k-1}, \quad (35)$$

$$\hat{\mathbf{g}}_{4,k} = \hat{\mathbf{g}}_{4,k-1} + \mu_{\mathbf{g}_4} e_{\text{Im},k} \text{Im} [\mathbf{X}_k^T] \hat{\mathbf{h}}_{4,k-1}. \quad (36)$$

Computational complexity:

For the calculations of the errors and the update equations

$$N_{4\mathbb{R},1} = 2N_{2\mathbb{R},1} \quad (37)$$

or

$$N_{4\mathbb{R},2} = 2N_{2\mathbb{R},2} \quad (38)$$

RV scalar multiplications are necessary.

Remark:

Due to the use of four RV BL filters this method might be able to consider correlated signals, which, depending on the application, may yield a better performance. Still, there exist several reasons why the extension to the fully CV case should be investigated. The fully CV filters also improve the problem of the $2\mathbb{R}$ filter structure with correlated signals, they can be implemented with less computational complexity than the $4\mathbb{R}$ filter structure, in many practical applications they are a more natural representation of the real-world system, and often the mathematical representation can be more compact [31], [32]. Finally, it can be shown that many fully CV BL systems cannot be modeled using four RV BL filters.

For all filters utilizing a fully CV BL filter structure, as depicted in Figure 6, it will be necessary to calculate derivatives of RV cost functions with respect to CV coefficient vectors. This cannot be done in the classical sense, because RV functions are in general not holomorphic functions. This follows from the fact that they in general do not fulfill the Cauchy-Riemann differential equations [31], [32]. Hence, we use Wirtinger's calculus [37] to derive those gradients. These derivations can be done similarly as in [31], [32], [35], [36].

C. CV BL Wiener filter

Our investigations of fully CV BL filter structures begin with the CV BL WF. Note that in this section only wide sense stationary (WSS) signals are considered.

WFs use the mean squared error (MSE) cost function

$$J = \mathbb{E} [e_k e_k^*] \in \mathbb{R}, \quad (39)$$

with the error for the fully CV BL filter structure given as

$$e_k = y_k - \hat{\mathbf{h}}^H \mathbf{X}_k \hat{\mathbf{g}}. \quad (40)$$

Applying Wirtinger's calculus to derive the gradient of (39) with respect to $\hat{\mathbf{h}}$ produces

$$\frac{\partial J}{\partial \hat{\mathbf{h}}} = -\mathbf{R}_{\mathbf{X}_y}^* \hat{\mathbf{g}}^* + \mathbf{R}_{\mathbf{g}}^* \hat{\mathbf{h}}^*, \quad (41)$$

where $\mathbf{R}_{\mathbf{X}_y} = \mathbb{E} [\mathbf{X}_k y_k^*] \in \mathbb{C}^{L \times M}$ and $\mathbf{R}_{\mathbf{g}} = \mathbb{E} [\mathbf{X}_k \hat{\mathbf{g}} \hat{\mathbf{g}}^H \mathbf{X}_k^H] \in \mathbb{C}^{L \times L}$. Setting (41) to zero yields

$$\hat{\mathbf{h}} = \mathbf{R}_{\mathbf{g}}^{-1} \mathbf{R}_{\mathbf{X}_y} \hat{\mathbf{g}}. \quad (42)$$

Similarly, the gradient of (39) with respect to $\hat{\mathbf{g}}$ can be derived as

$$\frac{\partial J}{\partial \hat{\mathbf{g}}} = -\mathbf{R}_{\mathbf{X}_y}^T \hat{\mathbf{h}}^* + \mathbf{R}_{\mathbf{h}}^* \hat{\mathbf{g}}^*, \quad (43)$$

with $\mathbf{R}_{\mathbf{h}} = \mathbb{E} [\mathbf{X}_k^H \hat{\mathbf{h}} \hat{\mathbf{h}}^H \mathbf{X}_k] \in \mathbb{C}^{M \times M}$. Setting (43) to zero we obtain

$$\hat{\mathbf{g}} = \mathbf{R}_{\mathbf{h}}^{-1} \mathbf{R}_{\mathbf{X}_y}^H \hat{\mathbf{h}}. \quad (44)$$

It is easy to see, that (42) and (44) depend on each other. Such as in the RV case [13], this issue can be resolved by evaluating (42) and (44) in an alternating manner as

$$\hat{\mathbf{h}}_n = \mathbf{R}_{\mathbf{g},n-1}^{-1} \mathbf{R}_{\mathbf{X}_y} \hat{\mathbf{g}}_{n-1} \quad (45)$$

and

$$\hat{\mathbf{g}}_n = \mathbf{R}_{\mathbf{h},n}^{-1} \mathbf{R}_{\mathbf{X}_y}^H \hat{\mathbf{h}}_n, \quad (46)$$

with $\hat{\mathbf{h}}_n \in \mathbb{C}^L$, $\hat{\mathbf{g}}_n \in \mathbb{C}^M$, $\mathbf{R}_{\mathbf{g},n-1} = \mathbb{E} [\mathbf{X}_n \hat{\mathbf{g}}_{n-1} \hat{\mathbf{g}}_{n-1}^H \mathbf{X}_n^H] \in \mathbb{C}^{L \times L}$, $\mathbf{R}_{\mathbf{h},n} = \mathbb{E} [\mathbf{X}_n^H \hat{\mathbf{h}}_n \hat{\mathbf{h}}_n^H \mathbf{X}_n] \in \mathbb{C}^{M \times M}$, and n representing the iteration index.

Remark:

Similarly as it was shown in [13], the matrices $\mathbf{R}_{\mathbf{g},n-1}$ and $\mathbf{R}_{\mathbf{h},n}$ can be rewritten to

$$\mathbf{R}_{\mathbf{g},n-1} = (\hat{\mathbf{g}}_{n-1} \otimes \mathbf{I}^{L \times L})^T \mathbf{R}_{\tilde{\mathbf{x}}\tilde{\mathbf{x}}} (\hat{\mathbf{g}}_{n-1} \otimes \mathbf{I}^{L \times L})^* \quad (47)$$

and

$$\mathbf{R}_{\mathbf{h},n} = (\mathbf{I}^{M \times M} \otimes \hat{\mathbf{h}}_n)^T \mathbf{R}_{\tilde{\mathbf{x}}\tilde{\mathbf{x}}}^* (\mathbf{I}^{M \times M} \otimes \hat{\mathbf{h}}_n)^* \quad (48)$$

with the covariance matrix $\mathbf{R}_{\tilde{\mathbf{x}}\tilde{\mathbf{x}}} = \mathbb{E} [\tilde{\mathbf{x}}_k \tilde{\mathbf{x}}_k^H]$. Hence, to evaluate the CV BL WF it is necessary to know $\mathbf{R}_{\tilde{\mathbf{x}}\tilde{\mathbf{x}}}$ and $\mathbf{R}_{\mathbf{X}_y}$. If these statistical quantities are not available, they may be estimated in advance by

$$\hat{\mathbf{R}}_{\tilde{\mathbf{x}}\tilde{\mathbf{x}}} = \frac{1}{N} \sum_{i=1}^N \tilde{\mathbf{x}}_i \tilde{\mathbf{x}}_i^H \quad (49)$$

and

$$\hat{\mathbf{r}}_{\tilde{\mathbf{x}}y} = \frac{1}{N} \sum_{i=1}^N \tilde{\mathbf{x}}_i y_i^*, \quad (50)$$

where N is the number of samples used for the estimation and $\hat{\mathbf{R}}_{\mathbf{X}_y} = \text{mat}_M [\hat{\mathbf{r}}_{\tilde{\mathbf{x}}y}]$.

Note that $\hat{\mathbf{g}}_0 = \mathbf{0}$ is a bad choice for the initialization, because \mathbf{h}_1 would go towards infinity. If no prior knowledge about \mathbf{g} or \mathbf{h} is available, $\hat{\mathbf{g}}_0$ can be chosen randomly, but unequal to the zero vector.

Convergence:

By investigating the cost function (39), it is possible to show that alternately evaluating (45) and (46) can't increase the MSE, leading to convergence. Assuming statistical independent and identically distributed columns $\mathbf{x}_{i,k}$ of \mathbf{X}_k , the filter will converge after one iteration step, which is proven in the following. Utilizing this assumption the covariance matrix $\mathbf{R}_{\tilde{\mathbf{x}}\tilde{\mathbf{x}}}$ can be written as a block-diagonal matrix

$$\mathbf{R}_{\tilde{\mathbf{x}}\tilde{\mathbf{x}}} = \mathbf{I}^{M \times M} \otimes \mathbf{R}_{\mathbf{xx}}, \quad (51)$$

where $\mathbf{R}_{\mathbf{xx}} = \mathbb{E} [\mathbf{x}_{i,k} \mathbf{x}_{i,k}^H] \in \mathbb{C}^{L \times L}$. Inserting (51) in (47) yields

$$\mathbf{R}_{\mathbf{g},n-1} = \sum_{m=1}^M |\hat{g}_{n-1,m}|^2 \mathbf{R}_{\mathbf{xx}}, \quad (52)$$

with $\hat{g}_{n-1,m}$ as the m th element of $\hat{\mathbf{g}}_{n-1}$. Inserting (7) into the definition of $\mathbf{R}_{\mathbf{X}_y}$ leads to

$$\mathbf{R}_{\mathbf{X}_y} = \text{mat}_M [\mathbf{R}_{\tilde{\mathbf{x}}\tilde{\mathbf{x}}} \mathbf{f}^*] \quad (53)$$

$$= [g_1^* \mathbf{R}_{\mathbf{xx}} \mathbf{h} \quad \cdots \quad g_M^* \mathbf{R}_{\mathbf{xx}} \mathbf{h}]^T, \quad (54)$$

with g_m as the m th element of \mathbf{g} . By inserting (52) and (54) into (45), one obtains

$$\hat{\mathbf{h}}_n = \left(\sum_{i=1}^M |\hat{g}_{n-1,i}|^2 \mathbf{R}_{\mathbf{xx}} \right)^{-1} \left(\sum_{i=1}^M \hat{g}_{n-1,i} g_i^* \mathbf{R}_{\mathbf{xx}} \right) \mathbf{h}. \quad (55)$$

This can be simplified to

$$\hat{\mathbf{h}}_n = \frac{\mathbf{g}^H \hat{\mathbf{g}}_{n-1}}{\hat{\mathbf{g}}_{n-1}^H \hat{\mathbf{g}}_{n-1}} \mathbf{h}. \quad (56)$$

As next step we use $\hat{\mathbf{h}}_n$ to calculate

$$\hat{\mathbf{g}}_n = \mathbf{R}_{\mathbf{h},n}^{-1} \mathbf{R}_{\mathbf{X}_y}^H \hat{\mathbf{h}}_n. \quad (57)$$

Inserting (51) in (48) yields the diagonal matrix

$$\mathbf{R}_{\mathbf{h},n} = \hat{\mathbf{h}}_n^T \mathbf{R}_{\mathbf{xx}}^* \hat{\mathbf{h}}_n^* \mathbf{I}^{M \times M}. \quad (58)$$

With (54) and (58) the estimate $\hat{\mathbf{g}}_n$ follows to

$$\hat{\mathbf{g}}_n = \frac{\mathbf{h}^H \mathbf{R}_{\mathbf{xx}} \hat{\mathbf{h}}_n}{\hat{\mathbf{h}}_n^H \mathbf{R}_{\mathbf{xx}} \hat{\mathbf{h}}_n} \mathbf{g}. \quad (59)$$

Inserting (56) leads to

$$\hat{\mathbf{g}}_n = \frac{\hat{\mathbf{g}}_{n-1}^H \hat{\mathbf{g}}_{n-1}}{\hat{\mathbf{g}}_{n-1}^H \mathbf{g}} \mathbf{g}. \quad (60)$$

From (56) one can see that

$$\hat{\mathbf{h}}_1 = \underbrace{\frac{\mathbf{g}^H \hat{\mathbf{g}}_0}{\hat{\mathbf{g}}_0^H \hat{\mathbf{g}}_0}}_{\nu} \mathbf{h} \quad (61)$$

is already a scaled version of the true but unknown vector \mathbf{h} . Moreover, since it is only possible to estimate \mathbf{h} up to a CV scalar, this is already the best estimate possible. Further, the first estimate

$$\hat{\mathbf{g}}_1 = \frac{1}{\nu^*} \mathbf{g} \quad (62)$$

is also already a scaled version of \mathbf{g} . Consequently, it is easy to see, that the Kronecker product produces the true equivalent linear coefficient vector:

$$\hat{\mathbf{g}}_1 \otimes \hat{\mathbf{h}}_1^* = \mathbf{f}. \quad (63)$$

The proof continues by showing that the sequences do not change for $n > 1$, i.e. $\hat{\mathbf{h}}_n = \hat{\mathbf{h}}_1$ and $\hat{\mathbf{g}}_n = \hat{\mathbf{g}}_1$ for $n \geq 1$. From (56), it is easy to see, that if $\hat{\mathbf{g}}_{n-1} = \frac{1}{\nu^*} \mathbf{g}$, then

$$\hat{\mathbf{h}}_n = \nu \mathbf{h}. \quad (64)$$

Similarly, from (60) one can see that

$$\hat{\mathbf{g}}_n = \frac{1}{\nu^*} \mathbf{g}. \quad (65)$$

Hence, convergence is reached after one iteration step. A final summary of the CV BL WF is given in Algorithm 1.

Note that if $\mathbf{R}_{\mathbf{xx}}$ does not fulfill (51), $\hat{\mathbf{h}}_1$ and $\hat{\mathbf{g}}_1$ would not just be scaled versions of \mathbf{h} and \mathbf{g} . Because of that, in the general case, the CV BL WF does not converge after one iteration step. Similarly, if the statistical properties $\mathbf{R}_{\mathbf{xx}}$ or $\mathbf{R}_{\mathbf{X}_y}$ are not known and therefore have to be estimated, convergence in one iteration step is not possible. A second way to handle unknown statistics is by implicitly estimating them using the LS approach as shown in the following chapter.

D. CV BL LS filter

Similarly to the linear LS filter, the CV BL LS filter does not require knowledge of any statistical signal properties. The corresponding cost function is

$$J = \sum_{i=1}^N e_i e_i^*, \quad (66)$$

where N data-points $\{y_i, \mathbf{X}_i\}$ have to be collected during a training phase. Similarly as for the CV BL WF, the gradient of (66) with respect to $\hat{\mathbf{h}}$ produces

$$\frac{\partial J}{\partial \hat{\mathbf{h}}} = \sum_{i=1}^N -y_i \mathbf{X}_i^* \hat{\mathbf{g}}^* + \mathbf{X}_i^* \hat{\mathbf{g}}^* \hat{\mathbf{g}}^T \mathbf{X}_i^T \hat{\mathbf{h}}^*. \quad (67)$$

Algorithm 1: CV BL WF*Initialize variables:* $\hat{\mathbf{g}}_0 \neq \mathbf{0}$ **for** $n = 1, 2, 3, \dots$ **do***Parameter update of $\hat{\mathbf{h}}_n$:*

$$\mathbf{R}_{\mathbf{g},n-1} = (\hat{\mathbf{g}}_{n-1} \otimes \mathbf{I}^{L \times L})^T \mathbf{R}_{\tilde{\mathbf{x}}\tilde{\mathbf{x}}} (\hat{\mathbf{g}}_{n-1} \otimes \mathbf{I}^{L \times L})^*$$

$$\hat{\mathbf{h}}_n = \mathbf{R}_{\mathbf{g},n-1}^{-1} \mathbf{R}_{\mathbf{x}y} \hat{\mathbf{g}}_{n-1}$$

Parameter update of $\hat{\mathbf{g}}_n$:

$$\mathbf{R}_{\mathbf{h},n} = (\mathbf{I}^{M \times M} \otimes \hat{\mathbf{h}}_n)^T \mathbf{R}_{\tilde{\mathbf{x}}\tilde{\mathbf{x}}}^* (\mathbf{I}^{M \times M} \otimes \hat{\mathbf{h}}_n)^*$$

$$\hat{\mathbf{g}}_n = \mathbf{R}_{\mathbf{h},n}^{-1} \mathbf{R}_{\mathbf{x}y}^H \hat{\mathbf{h}}_n$$

end**Algorithm 2: CV BL LS filter***Initialize variables:* $\hat{\mathbf{g}}_0 \neq \mathbf{0}$ **for** $n = 1, 2, 3, \dots$ **do***Parameter update of $\hat{\mathbf{h}}_n$:*

$$\hat{\mathbf{h}}_n = \left(\sum_{i=1}^N \mathbf{X}_i \hat{\mathbf{g}}_{n-1} \hat{\mathbf{g}}_{n-1}^H \mathbf{X}_i^H \right)^{-1} \sum_{i=1}^N y_i^* \mathbf{X}_i \hat{\mathbf{g}}_{n-1}$$

Parameter update of $\hat{\mathbf{g}}_n$:

$$\hat{\mathbf{g}}_n = \left(\sum_{i=1}^N \mathbf{X}_i^H \hat{\mathbf{h}}_n \hat{\mathbf{h}}_n^H \mathbf{X}_i \right)^{-1} \sum_{i=1}^N y_i \mathbf{X}_i^H \hat{\mathbf{h}}_n$$

end

Equating this gradient to zero yields

$$\hat{\mathbf{h}} = \left(\sum_{i=1}^N \mathbf{X}_i \hat{\mathbf{g}} \hat{\mathbf{g}}^H \mathbf{X}_i^H \right)^{-1} \sum_{i=1}^N y_i^* \mathbf{X}_i \hat{\mathbf{g}}. \quad (68)$$

Analogously, the gradient of (66) with respect to $\hat{\mathbf{g}}$ is

$$\frac{\partial J}{\partial \hat{\mathbf{g}}} = \sum_{i=1}^N -y_i^* \mathbf{X}_i^T \hat{\mathbf{h}}^* + \mathbf{X}_i^T \hat{\mathbf{h}}^* \hat{\mathbf{h}}^T \mathbf{X}_i^* \hat{\mathbf{g}}^*, \quad (69)$$

which yields

$$\hat{\mathbf{g}} = \left(\sum_{i=1}^N \mathbf{X}_i^H \hat{\mathbf{h}} \hat{\mathbf{h}}^H \mathbf{X}_i \right)^{-1} \sum_{i=1}^N y_i \mathbf{X}_i^H \hat{\mathbf{h}}. \quad (70)$$

Again, alternately evaluating (68) and (70) leads to the final update equations

$$\hat{\mathbf{h}}_n = \left(\sum_{i=1}^N \mathbf{X}_i \hat{\mathbf{g}}_{n-1} \hat{\mathbf{g}}_{n-1}^H \mathbf{X}_i^H \right)^{-1} \sum_{i=1}^N y_i^* \mathbf{X}_i \hat{\mathbf{g}}_{n-1} \quad (71)$$

and

$$\hat{\mathbf{g}}_n = \left(\sum_{i=1}^N \mathbf{X}_i^H \hat{\mathbf{h}}_n \hat{\mathbf{h}}_n^H \mathbf{X}_i \right)^{-1} \sum_{i=1}^N y_i \mathbf{X}_i^H \hat{\mathbf{h}}_n, \quad (72)$$

depicted in Algorithm 2.

Remark:

Similarly as for the CV BL WF, by investigating the cost function (66), it is possible to show that alternately evaluating (71) and (72) can't increase the costs in each iteration, leading to convergence.

Furthermore, it is easy to show, that the CV BL LS filter is mathematically identical to the CV BL WF when using the estimates (49) and (50) for $\hat{\mathbf{R}}_{\tilde{\mathbf{x}}\tilde{\mathbf{x}}}$ and $\hat{\mathbf{r}}_{\tilde{\mathbf{x}}y}$, respectively.

E. CV BL LMS filter

In this section, the CV BL LMS filter is derived. With the error signal

$$e_k = y_k - \hat{y}_k \quad (73)$$

$$= y_k - \hat{\mathbf{h}}_{k-1}^H \mathbf{X}_k \hat{\mathbf{g}}_{k-1}, \quad (74)$$

the ISE

$$J_k = e_k e_k^* \quad (75)$$

is now applied as a cost function. Application of a gradient descent method yields

$$\hat{\mathbf{h}}_k = \hat{\mathbf{h}}_{k-1} - \mu_{\mathbf{h}} \frac{\partial J_k}{\partial \hat{\mathbf{h}}_{k-1}^*} \quad (76)$$

and

$$\hat{\mathbf{g}}_k = \hat{\mathbf{g}}_{k-1} - \mu_{\mathbf{g}} \frac{\partial J_k}{\partial \hat{\mathbf{g}}_{k-1}^*}. \quad (77)$$

where $\mu_{\mathbf{h}}, \mu_{\mathbf{g}} \in \mathbb{R}$ are the step-sizes. Similarly as in Section III-C, the gradients of (75) with respect to $\hat{\mathbf{h}}_{k-1}^*$ and $\hat{\mathbf{g}}_{k-1}^*$ can be derived as

$$\frac{\partial J_k}{\partial \hat{\mathbf{h}}_{k-1}^*} = -e_k^* \mathbf{X}_k \hat{\mathbf{g}}_{k-1} \quad (78)$$

and

$$\frac{\partial J_k}{\partial \hat{\mathbf{g}}_{k-1}^*} = -e_k \mathbf{X}_k^H \hat{\mathbf{h}}_{k-1}, \quad (79)$$

respectively. Inserting (78) and (79) in (76) and (77), delivers the final update equations

$$\hat{\mathbf{h}}_k = \hat{\mathbf{h}}_{k-1} + \mu_{\mathbf{h}} e_k^* \mathbf{X}_k \hat{\mathbf{g}}_{k-1} \quad (80)$$

and

$$\hat{\mathbf{g}}_k = \hat{\mathbf{g}}_{k-1} + \mu_{\mathbf{g}} e_k \mathbf{X}_k^H \hat{\mathbf{h}}_{k-1}. \quad (81)$$

Computational complexity:

Exploiting the fact that multiplications of CV scalars can be done with three RV scalar multiplications [38], it is possible to compute (80) and (81) with

$$N_{\mathbb{C},1} = 9LM + 6M + 3L + 4 \quad (82)$$

or

$$N_{\mathbb{C},2} = 9LM + 3M + 6L + 4 \quad (83)$$

RV scalar multiplications, which are less than in (37) and (38).

Convergence:

In the following, similarly as in the RV case [15] and again assuming (51) with $\mathbf{R}_{\mathbf{xx}} = \sigma_x^2 \mathbf{I}^{L \times L}$, step-size boundaries will be derived in order to guarantee convergence. Therefore, with a scalar $\nu \in \mathbb{C}$, the error vectors

$$\Delta \mathbf{h}_k = \nu \mathbf{h} - \hat{\mathbf{h}}_k \quad (84)$$

and

$$\Delta \mathbf{g}_k = \frac{1}{\nu^*} \mathbf{g} - \hat{\mathbf{g}}_k, \quad (85)$$

are introduced. These errors show the difference between the current estimates $\hat{\mathbf{h}}_k$ and $\hat{\mathbf{g}}_k$ and scaled versions of the true vectors \mathbf{h} and \mathbf{g} , respectively. Inserting (80) into (84) yields

$$\Delta \mathbf{h}_k = \Delta \mathbf{h}_{k-1} - \mu_{\mathbf{h}} e_k^* \mathbf{X}_k \hat{\mathbf{g}}_{k-1}. \quad (86)$$

Calculating the second order moment of $||\Delta \mathbf{h}_k||$ results in

$$\mathbb{E} [||\Delta \mathbf{h}_k||^2] = \mathbb{E} [||\Delta \mathbf{h}_{k-1}||^2] - 2\mu_{\mathbf{h}} \mathbb{E} [\text{Re} [e_k \hat{\mathbf{g}}_{k-1}^H \mathbf{X}_k^H \Delta \mathbf{h}_{k-1}]] + \mu_{\mathbf{h}}^2 \mathbb{E} [|e_k|^2 \hat{\mathbf{g}}_{k-1}^H \mathbf{X}_k^H \mathbf{X}_k \hat{\mathbf{g}}_{k-1}]. \quad (87)$$

For a more compact notation

$$a_{\mathbf{h},k} = \mathbb{E} [\text{Re} [e_k \hat{\mathbf{g}}_{k-1}^H \mathbf{X}_k^H \Delta \mathbf{h}_{k-1}]] \quad (88)$$

and

$$b_{\mathbf{h},k} = \mathbb{E} [|e_k|^2 \hat{\mathbf{g}}_{k-1}^H \mathbf{X}_k^H \mathbf{X}_k \hat{\mathbf{g}}_{k-1}] \quad (89)$$

are introduced, which simplifies (87) to

$$\mathbb{E} [||\Delta \mathbf{h}_k||^2] = \mathbb{E} [||\Delta \mathbf{h}_{k-1}||^2] - 2\mu_{\mathbf{h}} a_{\mathbf{h},k} + \mu_{\mathbf{h}}^2 b_{\mathbf{h},k} . \quad (90)$$

By inserting (74) and (3) in (88), and assuming statistical independence between the noise n_k and the input signal matrix \mathbf{X}_k , (88) can be simplified to

$$a_{\mathbf{h},k} = \text{Re} \left[\mathbb{E} [\mathbf{h}^H \mathbf{X}_k \hat{\mathbf{g}}_{k-1}^H \mathbf{X}_k^H \Delta \mathbf{h}_{k-1}] - \mathbb{E} [\hat{\mathbf{h}}_{k-1}^H \mathbf{X}_k \hat{\mathbf{g}}_{k-1} \hat{\mathbf{g}}_{k-1}^H \mathbf{X}_k^H \Delta \mathbf{h}_{k-1}] \right] . \quad (91)$$

Further, using reformulated versions of (84) and (85) leads to

$$a_{\mathbf{h},k} = \text{Re} \left[\mathbb{E} [\nu^* \mathbf{h}^H \mathbf{X}_k \Delta \mathbf{g}_{k-1} \hat{\mathbf{g}}_{k-1}^H \mathbf{X}_k^H \Delta \mathbf{h}_{k-1}] + \mathbb{E} [\Delta \mathbf{h}_{k-1}^H \mathbf{X}_k \hat{\mathbf{g}}_{k-1} \hat{\mathbf{g}}_{k-1}^H \mathbf{X}_k^H \Delta \mathbf{h}_{k-1}] \right] . \quad (92)$$

Now, by incorporating (51) with $\mathbf{R}_{\mathbf{xx}} = \sigma_x^2 \mathbf{I}^{L \times L}$, this can be further simplified to

$$a_{\mathbf{h},k} = \text{Re} [\nu^* \sigma_x^2 \mathbf{h}^H \mathbb{E} [\Delta \mathbf{h}_{k-1}] \mathbb{E} [\hat{\mathbf{g}}_{k-1}^H \Delta \mathbf{g}_{k-1}]] + \sigma_x^2 \mathbb{E} [||\hat{\mathbf{g}}_{k-1}||^2] \mathbb{E} [||\Delta \mathbf{h}_{k-1}||^2] . \quad (93)$$

Using the approximation $\hat{\mathbf{g}}_{k-1}^H \mathbf{X}_k^H \mathbf{X}_k \hat{\mathbf{g}}_{k-1} \approx L \sigma_x^2 \mathbb{E} [||\hat{\mathbf{g}}_{k-1}||^2]$, (89) can be rewritten to

$$b_{\mathbf{h},k} = L \sigma_x^2 \mathbb{E} [||\hat{\mathbf{g}}_{k-1}||^2] \mathbb{E} [|e_k|^2] . \quad (94)$$

Similar reformulations as above can be applied, which yields

$$b_{\mathbf{h},k} = L \sigma_x^2 \mathbb{E} [||\hat{\mathbf{g}}_{k-1}||^2] (\sigma_n^2 + |\nu|^2 \sigma_x^2 ||\mathbf{h}||^2 \mathbb{E} [||\Delta \mathbf{g}_{k-1}||^2] + 2 \text{Re} [\nu \sigma_x^2 \mathbb{E} [\Delta \mathbf{h}_{k-1}^H] \mathbf{h} \mathbb{E} [\Delta \mathbf{g}_{k-1}^H \hat{\mathbf{g}}_{k-1}]] + \sigma_x^2 \mathbb{E} [||\hat{\mathbf{g}}_{k-1}||^2] \mathbb{E} [||\Delta \mathbf{h}_{k-1}||^2]) . \quad (95)$$

Inserting (93) and (95) into (90) yields

$$\mathbb{E} [||\Delta \mathbf{h}_k||^2] = \mathbb{E} [||\Delta \mathbf{h}_{k-1}||^2] c_{\mathbf{h},k} + d_{\mathbf{h},k} \quad (96)$$

where

$$c_{\mathbf{h},k} = 1 - 2\mu_{\mathbf{h}} \sigma_x^2 \mathbb{E} [||\hat{\mathbf{g}}_{k-1}||^2] + \mu_{\mathbf{h}}^2 \sigma_x^4 L \mathbb{E} [||\hat{\mathbf{g}}_{k-1}||^2]^2 \quad (97)$$

and

$$d_{\mathbf{h},k} = \mu_{\mathbf{h}}^2 L \sigma_x^2 \mathbb{E} [||\hat{\mathbf{g}}_{k-1}||^2] \left(\sigma_n^2 + |\nu|^2 \sigma_x^2 ||\mathbf{h}||^2 \mathbb{E} [||\Delta \mathbf{g}_{k-1}||^2] + 2 \text{Re} \left[\nu \sigma_x^2 \mathbb{E} [\Delta \mathbf{h}_{k-1}^H] \mathbf{h} \mathbb{E} [\Delta \mathbf{g}_{k-1}^H \hat{\mathbf{g}}_{k-1}] \right] \right) - 2\mu_{\mathbf{h}} \text{Re} [\nu^* \sigma_x^2 \mathbf{h}^H \mathbb{E} [\Delta \mathbf{h}_{k-1}] \mathbb{E} [\hat{\mathbf{g}}_{k-1} \Delta \mathbf{g}_{k-1}]] . \quad (98)$$

Note that $c_{\mathbf{h},k} > 0$, and to guarantee stability of the algorithm $c_{\mathbf{h},k} < 1$ should hold. With that, the boundaries

$$0 < \mu_{\mathbf{h}} < \frac{2}{L \sigma_x^2 \mathbb{E} [||\hat{\mathbf{g}}_{k-1}||^2]} \quad (99)$$

can be found. With similar arguments

$$\mathbb{E} [||\Delta \mathbf{g}_k||^2] = \mathbb{E} [||\Delta \mathbf{g}_{k-1}||^2] c_{\mathbf{g},k} + d_{\mathbf{g},k} \quad (100)$$

can be derived, where

$$c_{\mathbf{g},k} = 1 - 2\mu_{\mathbf{g}} \sigma_x^2 \mathbb{E} [||\hat{\mathbf{h}}_{k-1}||^2] + \mu_{\mathbf{g}}^2 \sigma_x^4 M \mathbb{E} [||\hat{\mathbf{h}}_{k-1}||^2]^2 \quad (101)$$

and

$$d_{\mathbf{g},k} = \mu_{\mathbf{g}}^2 M \sigma_x^2 \mathbb{E} [||\hat{\mathbf{h}}_{k-1}||^2] \left(\sigma_n^2 + \frac{1}{|\nu|^2} \sigma_x^2 ||\mathbf{g}||^2 \mathbb{E} [||\Delta \mathbf{h}_{k-1}||^2] + 2 \text{Re} \left[\frac{1}{\nu} \sigma_x^2 \mathbb{E} [\hat{\mathbf{h}}_{k-1}^H \Delta \mathbf{h}_{k-1}] \mathbf{g}^H \mathbb{E} [\Delta \mathbf{g}_{k-1}] \right] \right) - 2\mu_{\mathbf{g}} \text{Re} [\nu^* \sigma_x^2 \mathbf{h}^H \mathbb{E} [\Delta \mathbf{h}_{k-1}] \mathbb{E} [\hat{\mathbf{g}}_{k-1} \Delta \mathbf{g}_{k-1}]] . \quad (102)$$

Again it can be seen that $c_{\mathbf{g},k} > 0$, and for stability $c_{\mathbf{g},k} < 1$ should hold, which yields

$$0 < \mu_{\mathbf{g}} < \frac{2}{M \sigma_x^2 \mathbb{E} [||\hat{\mathbf{h}}_{k-1}||^2]} . \quad (103)$$

Algorithm 3: CV BL LMS filter

Initialize variables:

$$0 < \mu_{\mathbf{h}} < \frac{2}{L\sigma_x^2 \mathbb{E}[\|\hat{\mathbf{g}}_{k-1}\|^2]}$$

$$0 < \mu_{\mathbf{g}} < \frac{2}{M\sigma_x^2 \mathbb{E}[\|\hat{\mathbf{h}}_{k-1}\|^2]}$$

With $\mu_{\mathbf{h}}$ and $\mu_{\mathbf{g}}$ such that $\Delta \neq 0$

$\hat{\mathbf{h}}_0 \neq \mathbf{0}$ and $\hat{\mathbf{g}}_0 \neq \mathbf{0}$

for $k = 1, 2, 3, \dots$ **do**

$$e_k = y_k - \hat{\mathbf{h}}_{k-1}^H \mathbf{X}_k \hat{\mathbf{g}}_{k-1}$$

Parameter update of $\hat{\mathbf{h}}_k$:

$$\hat{\mathbf{h}}_k = \hat{\mathbf{h}}_{k-1} + \mu_{\mathbf{h}} e_k^* \mathbf{X}_k \hat{\mathbf{g}}_{k-1}$$

Parameter update of $\hat{\mathbf{g}}_k$:

$$\hat{\mathbf{g}}_k = \hat{\mathbf{g}}_{k-1} + \mu_{\mathbf{g}} e_k \mathbf{X}_k^H \hat{\mathbf{h}}_{k-1}$$

end

To analyze the algorithm after convergence, the terms

$$\mathbb{E} [\|\Delta \mathbf{h}_{\infty}\|^2] = \lim_{k \rightarrow \infty} \mathbb{E} [\|\Delta \mathbf{h}_k\|^2] \quad (104)$$

and

$$\mathbb{E} [\|\Delta \mathbf{g}_{\infty}\|^2] = \lim_{k \rightarrow \infty} \mathbb{E} [\|\Delta \mathbf{g}_k\|^2] \quad (105)$$

will be investigated. Assuming appropriate step-sizes,

$$\begin{aligned} \mathbb{E} [\|\Delta \mathbf{h}_{\infty}\|^2] &= \lim_{k \rightarrow \infty} \frac{d_{\mathbf{h},k}}{1 - c_{\mathbf{h},k}} \\ &= \frac{\mu_{\mathbf{h}} L \sigma_n^2 + \mu_{\mathbf{h}} L \sigma_x^2 |\nu|^2 \|\mathbf{h}\|^2 \mathbb{E} [\|\Delta \mathbf{g}_{\infty}\|^2]}{2 - \mu_{\mathbf{h}} \sigma_x^2 L \frac{1}{|\nu|^2} \|\mathbf{g}\|^2} \end{aligned} \quad (106)$$

and

$$\begin{aligned} \mathbb{E} [\|\Delta \mathbf{g}_{\infty}\|^2] &= \lim_{k \rightarrow \infty} \frac{d_{\mathbf{g},k}}{1 - c_{\mathbf{g},k}} \\ &= \frac{\mu_{\mathbf{g}} M \sigma_n^2 + \mu_{\mathbf{g}} M \sigma_x^2 \frac{1}{|\nu|^2} \|\mathbf{g}\|^2 \mathbb{E} [\|\Delta \mathbf{h}_{\infty}\|^2]}{2 - \mu_{\mathbf{g}} \sigma_x^2 M |\nu|^2 \|\mathbf{h}\|^2} \end{aligned} \quad (107)$$

can be obtained. With (106), (107), and some additional reformulations

$$\mathbb{E} [\|\Delta \mathbf{h}_{\infty}\|^2] = \frac{\mu_{\mathbf{h}} L \sigma_n^2}{\Delta} \quad (108)$$

and

$$\mathbb{E} [\|\Delta \mathbf{g}_{\infty}\|^2] = \frac{\mu_{\mathbf{g}} M \sigma_n^2}{\Delta}, \quad (109)$$

with $\Delta = 2 - \sigma_x^2 \left(\mu_{\mathbf{h}} L \frac{1}{|\nu|^2} \|\mathbf{g}\|^2 + \mu_{\mathbf{g}} M |\nu|^2 \|\mathbf{h}\|^2 \right)$, can be derived. Clearly, Δ has to be greater than zero, which yields an additional restriction for the step-sizes, in order to guarantee convergence on the mean. In Algorithm 3 the final CV BL LMS filter is depicted.

F. CV BL NLMS filter

One way to derive the NLMS algorithm is to set the a-posteriori error of the adaptive filter to zero, and to derive the step-size from this condition [17]. Having this in mind we introduce the a-posteriori errors

$$\bar{e}_k = y_k - \hat{\mathbf{h}}_k^H \mathbf{X}_k \hat{\mathbf{g}}_{k-1} \quad (110)$$

and

$$\tilde{e}_k = y_k - \hat{\mathbf{h}}_{k-1}^H \mathbf{X}_k \hat{\mathbf{g}}_k. \quad (111)$$

Algorithm 4: CV BL NLMS filter

Initialize variables:

$0 < \alpha_{\mathbf{h}} < 2$ and $0 < \alpha_{\mathbf{g}} < 2$ with $\alpha_{\mathbf{h}} + \alpha_{\mathbf{g}} < 2$

$\delta_{\mathbf{h}} > 0$ and $\delta_{\mathbf{g}} > 0$

$\hat{\mathbf{h}}_0 \neq \mathbf{0}$ and $\hat{\mathbf{g}}_0 \neq \mathbf{0}$

for $k = 1, 2, 3, \dots$ **do**

$e_k = y_k - \hat{\mathbf{h}}_{k-1}^H \mathbf{X}_k \hat{\mathbf{g}}_{k-1}$

Parameter update of $\hat{\mathbf{h}}_k$:

$$\hat{\mathbf{h}}_k = \hat{\mathbf{h}}_{k-1} + \frac{\alpha_{\mathbf{h}} \mathbf{X}_k \hat{\mathbf{g}}_{k-1}}{\delta_{\mathbf{h}} + \hat{\mathbf{g}}_{k-1}^H \mathbf{X}_k^H \mathbf{X}_k \hat{\mathbf{g}}_{k-1}} e_k^*$$

Parameter update of $\hat{\mathbf{g}}_k$:

$$\hat{\mathbf{g}}_k = \hat{\mathbf{g}}_{k-1} + \frac{\alpha_{\mathbf{g}} \mathbf{X}_k^H \hat{\mathbf{h}}_{k-1}}{\delta_{\mathbf{g}} + \hat{\mathbf{h}}_{k-1}^H \mathbf{X}_k \mathbf{X}_k^H \hat{\mathbf{h}}_{k-1}} e_k$$

end

Inserting (80) and (81) into (110) and (111) yields

$$\bar{e}_k = e_k \left(1 - \mu_{\mathbf{h}} \hat{\mathbf{g}}_{k-1}^H \mathbf{X}_k^H \mathbf{X}_k \hat{\mathbf{g}}_{k-1} \right) \quad (112)$$

and

$$\tilde{e}_k = e_k \left(1 - \mu_{\mathbf{g}} \hat{\mathbf{h}}_{k-1}^H \mathbf{X}_k \mathbf{X}_k^H \hat{\mathbf{h}}_{k-1} \right). \quad (113)$$

Setting those a-posteriori errors to zero, and assuming that $e_k \neq 0$ yields the step-sizes

$$\mu_{\mathbf{h},k} = \frac{1}{\hat{\mathbf{g}}_{k-1}^H \mathbf{X}_k^H \mathbf{X}_k \hat{\mathbf{g}}_{k-1}} \quad (114)$$

and

$$\mu_{\mathbf{g},k} = \frac{1}{\hat{\mathbf{h}}_{k-1}^H \mathbf{X}_k \mathbf{X}_k^H \hat{\mathbf{h}}_{k-1}}. \quad (115)$$

Finally, in accordance with the corresponding procedure for the ordinary NLMS algorithm, the update equations for the CV BL NLMS filter can be formulated as

$$\hat{\mathbf{h}}_k = \hat{\mathbf{h}}_{k-1} + \frac{\alpha_{\mathbf{h}} \mathbf{X}_k \hat{\mathbf{g}}_{k-1}}{\delta_{\mathbf{h}} + \hat{\mathbf{g}}_{k-1}^H \mathbf{X}_k^H \mathbf{X}_k \hat{\mathbf{g}}_{k-1}} e_k^* \quad (116)$$

and

$$\hat{\mathbf{g}}_k = \hat{\mathbf{g}}_{k-1} + \frac{\alpha_{\mathbf{g}} \mathbf{X}_k^H \hat{\mathbf{h}}_{k-1}}{\delta_{\mathbf{g}} + \hat{\mathbf{h}}_{k-1}^H \mathbf{X}_k \mathbf{X}_k^H \hat{\mathbf{h}}_{k-1}} e_k, \quad (117)$$

where $\alpha_{\mathbf{h}} \in \mathbb{R}$ and $\alpha_{\mathbf{g}} \in \mathbb{R}$ denote the normalized step-sizes and $\delta_{\mathbf{h}} \in \mathbb{R}$ and $\delta_{\mathbf{g}} \in \mathbb{R}$ are regulation constants to prevent divisions by very small numbers.

Convergence:

By using the approximations $\hat{\mathbf{g}}_{k-1}^H \mathbf{X}_k^H \mathbf{X}_k \hat{\mathbf{g}}_{k-1} \approx L \sigma_x^2 \mathbb{E} [||\hat{\mathbf{g}}_{k-1}||^2]$ and $\hat{\mathbf{h}}_{k-1}^H \mathbf{X}_k \mathbf{X}_k^H \hat{\mathbf{h}}_{k-1} \approx M \sigma_x^2 \mathbb{E} [||\hat{\mathbf{h}}_{k-1}||^2]$ and comparing (114) and (115) with (99) and (103), it is easy to see that the stability boundaries for the normalized step-sizes result in

$$0 < \alpha_{\mathbf{h}} < 2 \quad (118)$$

and

$$0 < \alpha_{\mathbf{g}} < 2. \quad (119)$$

With the normalized step-sizes (114) and (115), Δ simplifies to $\Delta = 2 - (\alpha_{\mathbf{h}} + \alpha_{\mathbf{g}})$. Clearly, Δ has to be greater than zero, which yields

$$\alpha_{\mathbf{h}} + \alpha_{\mathbf{g}} < 2 \quad (120)$$

as an additional restriction for the normalized step-sizes, in order to guarantee convergence on the mean. Finally, Algorithm 4 summarizes the CV BL NLMS filter.

G. CV BL RLS filter

The cost function for the CV BL RLS is defined as

$$J_k = \sum_{i=1}^k \lambda^{k-i} \bar{e}_i \bar{e}_i^* \quad (121)$$

where $\bar{e}_i = y_i - \hat{\mathbf{h}}_k^H \mathbf{X}_i \hat{\mathbf{g}}_k$ and $\lambda \in \mathbb{R}$ is the forgetting factor. In a slowly varying system environment it may be assumed that $\hat{\mathbf{h}}_k^H \mathbf{X}_i \hat{\mathbf{g}}_k \approx \hat{\mathbf{h}}_k^H \mathbf{X}_i \hat{\mathbf{g}}_{i-1}$ when the index i is close to k . For $i \ll k$ the introduced error gets attenuated by λ^{k-i} [39]. To derive the first update equation for $\hat{\mathbf{h}}_k$ of the CV BL RLS filter, the cost function is approximated as

$$J_k \approx \sum_{i=1}^k \lambda^{k-i} \epsilon_i \epsilon_i^* \quad (122)$$

where $\epsilon_i = y_i - \hat{\mathbf{h}}_k^H \mathbf{X}_i \hat{\mathbf{g}}_{i-1}$. The gradient of (122) with respect to $\hat{\mathbf{h}}_k^*$ yields

$$\frac{\partial J_k}{\partial \hat{\mathbf{h}}_k^*} = \sum_{i=1}^k \lambda^{k-i} \mathbf{X}_i \hat{\mathbf{g}}_{i-1} \hat{\mathbf{g}}_{i-1}^H \mathbf{X}_i^H \hat{\mathbf{h}}_k - \sum_{i=1}^k \lambda^{k-i} y_i^* \mathbf{X}_i \hat{\mathbf{g}}_{i-1}. \quad (123)$$

Introducing

$$\tilde{\mathbf{R}}_{\mathbf{g},k} = \sum_{i=1}^k \lambda^{k-i} \mathbf{X}_i \hat{\mathbf{g}}_{i-1} \hat{\mathbf{g}}_{i-1}^H \mathbf{X}_i^H \in \mathbb{C}^{L \times L} \quad (124)$$

$$= \mathbf{X}_k \hat{\mathbf{g}}_{k-1} \hat{\mathbf{g}}_{k-1}^H \mathbf{X}_k^H + \lambda \tilde{\mathbf{R}}_{\mathbf{g},k-1} \quad (125)$$

and

$$\tilde{\mathbf{r}}_{\mathbf{g},k} = \sum_{i=1}^k \lambda^{k-i} y_i^* \mathbf{X}_i \hat{\mathbf{g}}_{i-1} \in \mathbb{C}^{L \times 1} \quad (126)$$

$$= y_k^* \mathbf{X}_k \hat{\mathbf{g}}_{k-1} + \lambda \tilde{\mathbf{r}}_{\mathbf{g},k-1}, \quad (127)$$

and setting (123) to zero yields

$$\hat{\mathbf{h}}_k = \tilde{\mathbf{R}}_{\mathbf{g},k}^{-1} \tilde{\mathbf{r}}_{\mathbf{g},k}. \quad (128)$$

Utilizing Woodbury's matrix identity [40] and renaming $\tilde{\mathbf{R}}_{\mathbf{g},k}^{-1}$ as $\mathbf{P}_{\mathbf{g},k}$ leads to

$$\mathbf{P}_{\mathbf{g},k} = \lambda^{-1} \mathbf{P}_{\mathbf{g},k-1} - \frac{\lambda^{-1} \mathbf{P}_{\mathbf{g},k-1} \mathbf{X}_k \hat{\mathbf{g}}_{k-1} \hat{\mathbf{g}}_{k-1}^H \mathbf{X}_k^H \mathbf{P}_{\mathbf{g},k-1}}{\lambda + \hat{\mathbf{g}}_{k-1}^H \mathbf{X}_k^H \mathbf{P}_{\mathbf{g},k-1} \mathbf{X}_k \hat{\mathbf{g}}_{k-1}}. \quad (129)$$

Subsequently, the gain vector

$$\mathbf{k}_{\mathbf{g},k} = \frac{\mathbf{P}_{\mathbf{g},k-1} \mathbf{X}_k \hat{\mathbf{g}}_{k-1}}{\lambda + \hat{\mathbf{g}}_{k-1}^H \mathbf{X}_k^H \mathbf{P}_{\mathbf{g},k-1} \mathbf{X}_k \hat{\mathbf{g}}_{k-1}} \in \mathbb{C}^L, \quad (130)$$

can be defined. After a few reformulations, (129) and (130) can be simplified to

$$\mathbf{P}_{\mathbf{g},k} = \lambda^{-1} (\mathbf{P}_{\mathbf{g},k-1} - \mathbf{k}_{\mathbf{g},k} \hat{\mathbf{g}}_{k-1}^H \mathbf{X}_k^H \mathbf{P}_{\mathbf{g},k-1}) \quad (131)$$

and

$$\mathbf{k}_{\mathbf{g},k} = \mathbf{P}_{\mathbf{g},k} \mathbf{X}_k \hat{\mathbf{g}}_{k-1}, \quad (132)$$

respectively. Incorporating (127) into (128) yields

$$\hat{\mathbf{h}}_k = y_k^* \mathbf{P}_{\mathbf{g},k} \mathbf{X}_k \hat{\mathbf{g}}_{k-1} + \lambda \mathbf{P}_{\mathbf{g},k} \mathbf{r}_{\mathbf{g},k-1}. \quad (133)$$

With (131) and (132) this can be rewritten to

$$\hat{\mathbf{h}}_k = y_k^* \mathbf{k}_{\mathbf{g},k} + (\mathbf{P}_{\mathbf{g},k-1} - \mathbf{k}_{\mathbf{g},k} \hat{\mathbf{g}}_{k-1}^H \mathbf{X}_k^H \mathbf{P}_{\mathbf{g},k-1}) \mathbf{r}_{\mathbf{g},k-1}. \quad (134)$$

Finally, (134) can be simplified to

$$\hat{\mathbf{h}}_k = \hat{\mathbf{h}}_{k-1} + e_k^* \mathbf{k}_{\mathbf{g},k}. \quad (135)$$

The next step is to perform the same steps for $\hat{\mathbf{g}}_k$ by utilizing the assumption $\hat{\mathbf{h}}_k^H \mathbf{X}_i \hat{\mathbf{g}}_k \approx \hat{\mathbf{h}}_{i-1}^H \mathbf{X}_i \hat{\mathbf{g}}_k$. The approximated cost function yields

$$J_k \approx \sum_{i=1}^k \lambda^{k-i} \epsilon_i \epsilon_i^* \quad (136)$$

where $\epsilon_i = y_i - \hat{\mathbf{h}}_{i-1}^H \mathbf{X}_i \hat{\mathbf{g}}_k$. The derivative of (136) with respect to $\hat{\mathbf{g}}_k^*$ yields

$$\frac{\partial J_k}{\partial \hat{\mathbf{g}}_k^*} = \sum_{i=1}^k \lambda^{k-i} \mathbf{X}_i^H \hat{\mathbf{h}}_{i-1} \hat{\mathbf{h}}_{i-1}^H \mathbf{X}_i \hat{\mathbf{g}}_k - \sum_{i=1}^k \lambda^{k-i} y_i \mathbf{X}_i^H \hat{\mathbf{h}}_{i-1}. \quad (137)$$

Similarly to the derivation above, we obtain

$$\hat{\mathbf{g}}_k = \tilde{\mathbf{R}}_{\mathbf{h},k}^{-1} \tilde{\mathbf{r}}_{\mathbf{h},k} \quad (138)$$

by introducing

$$\tilde{\mathbf{R}}_{\mathbf{h},k} = \sum_{i=1}^k \lambda^{k-i} \mathbf{X}_i^H \hat{\mathbf{h}}_{i-1} \hat{\mathbf{h}}_{i-1}^H \mathbf{X}_i \in \mathbb{R}^{M \times M} \quad (139)$$

$$= \mathbf{X}_k^H \hat{\mathbf{h}}_{k-1} \hat{\mathbf{h}}_{k-1}^H \mathbf{X}_k + \lambda \tilde{\mathbf{R}}_{\mathbf{h},k-1} \quad (140)$$

and

$$\tilde{\mathbf{r}}_{\mathbf{h},k} = \sum_{i=1}^k \lambda^{k-i} y_i \mathbf{X}_i^H \hat{\mathbf{h}}_{i-1} \in \mathbb{C}^{M \times 1} \quad (141)$$

$$= y_k \mathbf{X}_k^H \hat{\mathbf{h}}_{k-1} + \lambda \tilde{\mathbf{r}}_{\mathbf{h},k-1}^H. \quad (142)$$

Woodbury's matrix identity and renaming $\tilde{\mathbf{R}}_{\mathbf{h},k}^{-1}$ as $\mathbf{P}_{\mathbf{h},k}$ produce

$$\mathbf{P}_{\mathbf{h},k} = \lambda^{-1} \mathbf{P}_{\mathbf{h},k-1} - \frac{\lambda^{-1} \mathbf{P}_{\mathbf{h},k-1} \mathbf{X}_k^H \hat{\mathbf{h}}_{k-1} \hat{\mathbf{h}}_{k-1}^H \mathbf{X}_k \mathbf{P}_{\mathbf{h},k-1}}{\lambda + \hat{\mathbf{h}}_{k-1}^H \mathbf{X}_k \mathbf{P}_{\mathbf{h},k-1} \mathbf{X}_k^H \hat{\mathbf{h}}_{k-1}}. \quad (143)$$

By introducing a second gain vector

$$\mathbf{k}_{\mathbf{h},k} = \frac{\mathbf{P}_{\mathbf{h},k-1} \mathbf{X}_k^H \hat{\mathbf{h}}_{k-1}}{\lambda + \hat{\mathbf{h}}_{k-1}^H \mathbf{X}_k \mathbf{P}_{\mathbf{h},k-1} \mathbf{X}_k^H \hat{\mathbf{h}}_{k-1}} \in \mathbb{C}^M \quad (144)$$

(143) can be rewritten as

$$\mathbf{P}_{\mathbf{h},k} = \lambda^{-1} \left(\mathbf{P}_{\mathbf{h},k-1} - \mathbf{k}_{\mathbf{h},k} \hat{\mathbf{h}}_{k-1}^H \mathbf{X}_k \mathbf{P}_{\mathbf{h},k-1} \right). \quad (145)$$

Further, with (145) the gain vector can be reformulated as

$$\mathbf{k}_{\mathbf{h},k} = \mathbf{P}_{\mathbf{h},k} \mathbf{X}_k^H \hat{\mathbf{h}}_{k-1}. \quad (146)$$

Inserting (145), (146) and (142) into (138) yields the second update equation

$$\hat{\mathbf{g}}_k = \hat{\mathbf{g}}_{k-1} + e_k \mathbf{k}_{\mathbf{h},k}, \quad (147)$$

of the CV BL RLS filter. In Algorithm 5 the CV BL RLS filter is summarized.

H. Mixed CV-RV BL filter structure

For the sake of completeness, this section presents the results for the mixed CV-RV BL filter structure. Instead of the system in (3), a RV coefficient vector $\mathbf{g} \in \mathbb{R}^M$ is assumed. Except for the mixed CV-RV BL NLMS filter, the derivations of the following filters can be performed analogously to the ones above. Therefore, just the final update equations are presented in this section, while the derivation of the CV-RV BL NLMS filter can be found in the appendix.

Mixed CV-RV BL WF:

$$\hat{\mathbf{h}}_n = \mathbf{R}_{\mathbf{g},n-1}^{-1} \mathbf{R}_{\mathbf{X}y} \hat{\mathbf{g}}_{n-1} \quad (148)$$

$$\hat{\mathbf{g}}_n = \text{Re}[\mathbf{R}_{\mathbf{h},n}]^{-1} \text{Re}[\mathbf{R}_{\mathbf{X}y}^H \hat{\mathbf{h}}_n] \quad (149)$$

Algorithm 5: CV BL RLS filter

Initialize variables:

$\mathbf{P}_{\mathbf{g},0} = \nu_{\mathbf{g}} \mathbf{I}^{L \times L}$ with $\nu_{\mathbf{g}} > 0$

$\mathbf{P}_{\mathbf{h},0} = \nu_{\mathbf{h}} \mathbf{I}^{M \times M}$ with $\nu_{\mathbf{h}} > 0$

$0 < \lambda \leq 1$

$\hat{\mathbf{h}}_0 \neq \mathbf{0}$ and $\hat{\mathbf{g}}_0 \neq \mathbf{0}$

for $k = 1, 2, 3, \dots$ **do**

$e_k = y_k - \hat{\mathbf{h}}_{k-1}^H \mathbf{X}_k \hat{\mathbf{g}}_{k-1}$

Parameter update of $\hat{\mathbf{h}}_k$:

$\mathbf{k}_{\mathbf{g},k} = \frac{\mathbf{P}_{\mathbf{g},k-1} \mathbf{X}_k \hat{\mathbf{g}}_{k-1}}{\lambda + \hat{\mathbf{g}}_{k-1}^H \mathbf{X}_k^H \mathbf{P}_{\mathbf{g},k-1} \mathbf{X}_k \hat{\mathbf{g}}_{k-1}}$

$\mathbf{P}_{\mathbf{g},k} = \lambda^{-1} (\mathbf{P}_{\mathbf{g},k-1} - \mathbf{k}_{\mathbf{g},k} \hat{\mathbf{g}}_{k-1}^H \mathbf{X}_k^H \mathbf{P}_{\mathbf{g},k-1})$

$\hat{\mathbf{h}}_k = \hat{\mathbf{h}}_{k-1} + e_k^* \mathbf{k}_{\mathbf{g},k}$

Parameter update of $\hat{\mathbf{g}}_k$:

$\mathbf{k}_{\mathbf{h},k} = \frac{\mathbf{P}_{\mathbf{h},k-1} \mathbf{X}_k^H \hat{\mathbf{h}}_{k-1}}{\lambda + \hat{\mathbf{h}}_{k-1}^H \mathbf{X}_k \mathbf{P}_{\mathbf{h},k-1} \mathbf{X}_k^H \hat{\mathbf{h}}_{k-1}}$

$\mathbf{P}_{\mathbf{h},k} = \lambda^{-1} (\mathbf{P}_{\mathbf{h},k-1} - \mathbf{k}_{\mathbf{h},k} \hat{\mathbf{h}}_{k-1}^H \mathbf{X}_k \mathbf{P}_{\mathbf{h},k-1})$

$\hat{\mathbf{g}}_k = \hat{\mathbf{g}}_{k-1} + e_k \mathbf{k}_{\mathbf{h},k}$

end

Mixed CV-RV BL LS filter:

$$\hat{\mathbf{h}}_n = \left(\sum_{i=1}^N \mathbf{X}_i \hat{\mathbf{g}}_{n-1} \hat{\mathbf{g}}_{n-1}^H \mathbf{X}_i^H \right)^{-1} \sum_{i=1}^N y_i^* \mathbf{X}_i \hat{\mathbf{g}}_{n-1} \quad (150)$$

$$\hat{\mathbf{g}}_n = \left(\sum_{i=1}^N \text{Re} \left[\mathbf{X}_i^H \hat{\mathbf{h}}_n \hat{\mathbf{h}}_n^H \mathbf{X}_i \right] \right)^{-1} \sum_{i=1}^N \text{Re} \left[y_i \mathbf{X}_i^H \hat{\mathbf{h}}_n \right] \quad (151)$$

Mixed CV-RV BL LMS filter:

$$\hat{\mathbf{h}}_k = \hat{\mathbf{h}}_{k-1} + \mu_{\mathbf{h}} e_k^* \mathbf{X}_k \hat{\mathbf{g}}_{k-1} \quad (152)$$

$$\hat{\mathbf{g}}_k = \hat{\mathbf{g}}_{k-1} + \mu_{\mathbf{g}} 2 \text{Re} \left[e_k \mathbf{X}_k^H \hat{\mathbf{h}}_{k-1} \right] \quad (153)$$

Mixed CV-RV BL NLMS filter:

$$\hat{\mathbf{h}}_k = \hat{\mathbf{h}}_{k-1} + \frac{\alpha_{\mathbf{h}} \mathbf{X}_k \hat{\mathbf{g}}_{k-1}}{\delta_{\mathbf{h}} + \hat{\mathbf{g}}_{k-1}^T \mathbf{X}_k^H \mathbf{X}_k \hat{\mathbf{g}}_{k-1}} e_k^* \quad (154)$$

$$\hat{\mathbf{g}}_k = \hat{\mathbf{g}}_{k-1} + \alpha_{\mathbf{g}} 2 \text{Re} \left[e_k \mathbf{X}_k^H \hat{\mathbf{h}}_{k-1} \right] \frac{\text{Re} \left[e_k^* \hat{\mathbf{h}}_{k-1}^H \mathbf{X}_k \right] \text{Re} \left[e_k \mathbf{X}_k^H \hat{\mathbf{h}}_{k-1} \right]}{\delta_{\mathbf{g}} + \text{Re} \left[e_k \hat{\mathbf{h}}_{k-1}^T \mathbf{X}_k^* \right] \mathbf{X}_k^H \hat{\mathbf{h}}_{k-1} \hat{\mathbf{h}}_{k-1}^H \mathbf{X}_k \text{Re} \left[e_k \mathbf{X}_k^H \hat{\mathbf{h}}_{k-1} \right]} \quad (155)$$

Mixed CV-RV BL RLS filter:

$$\mathbf{k}_{\mathbf{g},k} = \frac{\mathbf{P}_{\mathbf{g},k-1} \mathbf{X}_k \hat{\mathbf{g}}_{k-1}}{\lambda + \hat{\mathbf{g}}_{k-1}^T \mathbf{X}_k^H \mathbf{P}_{\mathbf{g},k-1} \mathbf{X}_k \hat{\mathbf{g}}_{k-1}} \quad (156)$$

$$\mathbf{K}_{\mathbf{h},k} = \lambda^{-1} \tilde{\mathbf{P}}_{\mathbf{h},k-1} \tilde{\mathbf{X}}_k \left(\mathbf{I}^{2 \times 2} + \tilde{\mathbf{X}}_k^H \lambda^{-1} \tilde{\mathbf{P}}_{\mathbf{h},k-1} \tilde{\mathbf{X}}_k \right)^{-1} \quad (157)$$

$$\tilde{\mathbf{P}}_{\mathbf{h},k} = \mathbf{P}_{\mathbf{h},k} + \mathbf{P}_{\mathbf{h},k}^* \quad (158)$$

$$\tilde{\mathbf{X}}_k = [\mathbf{X}_k^H \hat{\mathbf{h}}_{k-1} \quad \mathbf{X}_k^T \hat{\mathbf{h}}_{k-1}^*] \quad (159)$$

$$\mathbf{P}_{\mathbf{g},k} = \lambda^{-1} (\mathbf{P}_{\mathbf{g},k-1} - \mathbf{k}_{\mathbf{g},k} \hat{\mathbf{g}}_{k-1}^T \mathbf{X}_k^H \mathbf{P}_{\mathbf{g},k-1}) \quad (160)$$

$$\tilde{\mathbf{P}}_{\mathbf{h},k} = \lambda^{-1} (\tilde{\mathbf{P}}_{\mathbf{h},k-1} - \mathbf{K}_{\mathbf{h},k} \tilde{\mathbf{X}}_k^H \tilde{\mathbf{P}}_{\mathbf{h},k-1}) \quad (161)$$

$$\hat{\mathbf{h}}_k = \hat{\mathbf{h}}_{k-1} + e_k^* \mathbf{k}_{\mathbf{g},k} \quad (162)$$

$$\hat{\mathbf{g}}_k = \hat{\mathbf{g}}_{k-1} + \mathbf{K}_{\mathbf{h},k} \mathbf{e}_k \quad (163)$$

IV. SIMULATION RESULTS

This section presents simulation results in the context of system identification. First, several simulations with MISO systems similar as in [13]–[22] are performed. Second, the identifications of nonlinear Hammerstein systems are regarded.

A. Identification of a MISO system

The input signal matrix is given by

$$\mathbf{X}_k = \begin{bmatrix} \mathbf{x}_k^T \\ \mathbf{x}_{k-1}^T \\ \vdots \\ \mathbf{x}_{k-L+1}^T \end{bmatrix}, \quad (164)$$

where $\mathbf{x}_k = [x_{1,k} \ x_{2,k} \ \cdots \ x_{M,k}]^T \in \mathbb{C}^M$ contains the M input samples of the MISO system, at a time-instance k , as can be seen in Figure 1.

1) *Bilinear versus linear approach:* As a first task we regard the identification of a MISO system of the form in (3), using both the CV BL NLMS and the CV linear NLMS filter. For the following simulation we chose, $M = 5$, $x_{m,k} \sim \mathcal{CN}(0, 1)$, and $n_k \sim \mathcal{CN}(0, 1)$. The initial values $\hat{\mathbf{h}}_0$ and $\hat{\mathbf{g}}_0$, as well as the true values \mathbf{h} and \mathbf{g} , are randomly chosen from a normal distribution with zero mean and a standard deviation of $\sigma = 10$. To observe the influence of the filter length, L has been increased from two to 30. Note that the lengths of $\hat{\mathbf{h}}_k$ and $\hat{\mathbf{g}}_k$ were chosen to be equal to the lengths of \mathbf{h} and \mathbf{g} , respectively. As explained in (8), it is only possible to estimate \mathbf{h} and \mathbf{g} up to a complex scalar. Therefore, the evaluation is performed on $\hat{\mathbf{f}}_k = \hat{\mathbf{g}}_k \otimes \hat{\mathbf{h}}_k^*$ using the normalized misalignment

$$NM(\hat{\mathbf{f}}_k) = \frac{\|\mathbf{f} - \hat{\mathbf{f}}_k\|_2^2}{\|\mathbf{f}\|_2^2} \in \mathbb{R}. \quad (165)$$

In Figure 7, the linear NLMS (left) and the BL NLMS (right) filters are compared, where $\alpha_{\mathbf{h}} = \alpha_{\mathbf{g}} = 0.7$, $\alpha_{\mathbf{f}} = 1$, and $\delta_{\mathbf{h}} = \delta_{\mathbf{g}} = \delta_{\mathbf{f}} = 10^{-2}$. $\alpha_{\mathbf{f}}$ and $\delta_{\mathbf{f}}$ are the parameters of the CV linear NLMS filter. All parameters were chosen to yield approximately the same steady state performance for all involved filters. As L increases, more iterations are required for convergence to the same level. However, it is evident that, especially for larger filter lengths, the BL filter converges much faster than the linear one. This is because the linear filter estimates LM unknown CV coefficients, whereas the BL filter just needs to estimate $L + M$ coefficients.

2) *CV BL WF versus CV BL LS filter:* In this section, simulations involving the proposed CV BL WF and the CV BL LS filter are presented. To demonstrate the behavior of those filters, we consider a filtering task similar to the one in the previous section. Note that for the CV BL WF, it is necessary to know the statistical properties $\mathbf{R}_{\tilde{\mathbf{x}}\tilde{\mathbf{x}}}$ and $\mathbf{R}_{\mathbf{X}_y}$. If these properties are not available, they may be estimated in advance with (49) and (50), or by using the CV BL LS filter. As above, a BL system of the form (3) with the same structure for the input signal matrix \mathbf{X}_k , with $L = 64$ and $M = 5$, is considered. The unknown vectors \mathbf{h} and \mathbf{g} , as well as the initial value $\hat{\mathbf{g}}_0$ were selected from the same random distribution as described above. For the first simulation in Figure 8, the statistical properties were assumed to be $\mathbf{R}_{\tilde{\mathbf{x}}\tilde{\mathbf{x}}} = \mathbf{I}^{320 \times 320}$ and $\mathbf{R}_{\mathbf{X}_y} = \text{mat}_M[\mathbf{R}_{\tilde{\mathbf{x}}\tilde{\mathbf{x}}} \mathbf{f}^*]$, where $x_{m,k}$ represents CV white Gaussian noise. Since $\hat{\mathbf{R}}_{\tilde{\mathbf{x}}\tilde{\mathbf{x}}}$ has to be invertible, the minimum number of data-points is $N = LM$. As described in Section III-C, the CV BL WF, with perfectly known statistics, converges in just one iteration step. However,

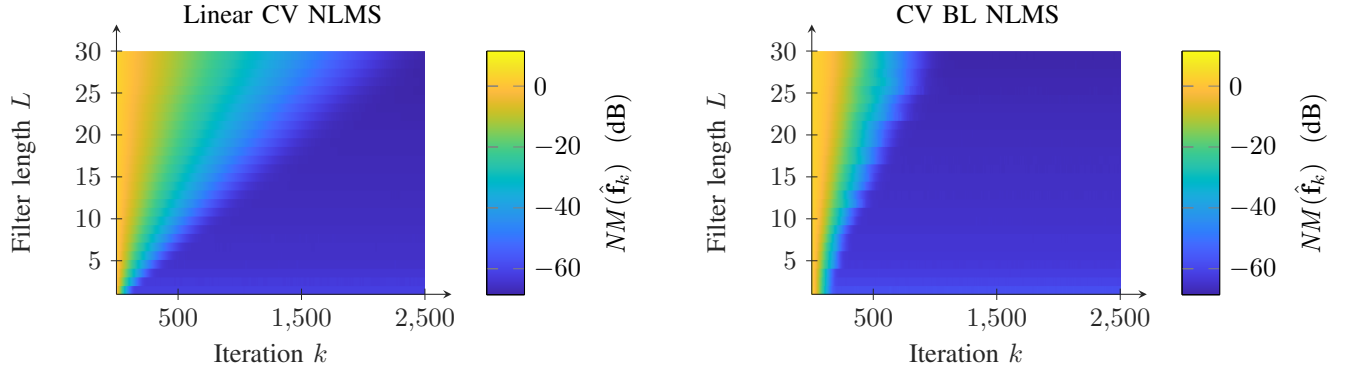


Fig. 7. The behavior of NLMS algorithms when varying L . Left: Linear CV NLMS. Right: CV BL NLMS. The colors represent the normalized misalignment (165) in dB.

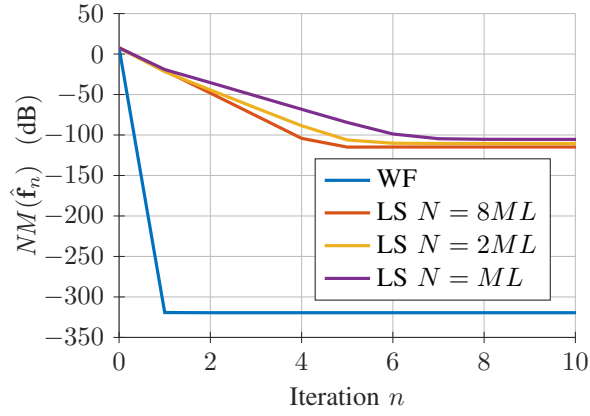


Fig. 8. Convergence curves of the CV BL WF and the CV BL LS filter using CV white Gaussian noise for the input signal.

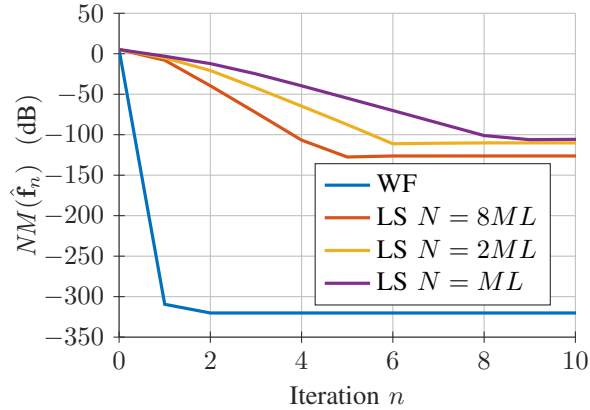


Fig. 9. Convergence curves of the CV BL WF and the CV BL LS filter using a CV moving average process for the input signal.

one can see that the CV BL LS filter does not converge in one iteration step, and using more data improves the estimation of $\mathbf{R}_{\tilde{x}\tilde{x}}$ and $\mathbf{R}_{\mathbf{x}y}$, resulting in faster and better convergence.

In Figure 9, instead of white Gaussian noise, a first-order moving average process is used. For this, proper CV Gaussian random signals $u_{m,k} \sim \mathcal{CN}(0, 0.5)$ are used to generate the input signals as $x_{m,k} = u_{m,k} + u_{m,k-1}$. Similar to the previous case, the result improves as the estimation of the statistical properties becomes more accurate. Furthermore, as mentioned in Section III-C, using the exact statistical properties leads to convergence in one iteration. Note that in Figure 9, it might appear otherwise, which can be attributed to the simulation accuracy of 64-bit floating-point arithmetic.

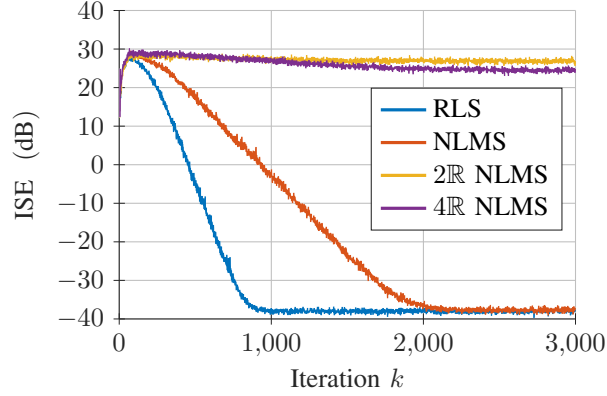


Fig. 10. Convergence behavior of the CV BL RLS filter, the CV BL NLMS filter, the 2 \mathbb{R} NLMS filter, and the 4 \mathbb{R} NLMS filter, when identifying a MISO system.

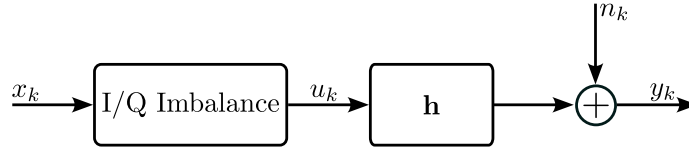


Fig. 11. Block diagram of a communication transmitter in combination with a linear channel.

3) *CV BL NLMS versus CV BL RLS versus 2 \mathbb{R} NLMS versus 4 \mathbb{R} NLMS*: In the next simulations we compare the CV BL RLS filter with the BL NLMS-based filters. This is done by identifying the same CV BL system as in the previous simulations. The input and noise signals are picked from complex random distributions $x_{m,k} \sim \mathcal{CN}(0, \sigma_x^2)$, $n_k \sim \mathcal{CN}(0, \sigma_n^2)$ with $\sigma_n = \sigma_x = 0.01$. To implement the CV BL NLMS filter, the normalized step-sizes and the regularization constants are chosen as $\alpha_h = \alpha_g = 0.5$ and $\delta_h = \delta_g = 10^{-4}$, respectively. For the initialization of the CV BL RLS filter $\mathbf{P}_{h,0} = 10\mathbf{I}^{M \times M}$, $\mathbf{P}_{g,0} = 10\mathbf{I}^{L \times L}$, and $\lambda = 1 - \frac{1}{L}$ were selected. The latter values were picked similarly to those in [18], while the values for the CV BL NLMS filter were selected to ensure that both filters achieve about the same level of normalized misalignment. Further, the parameters for the 2 \mathbb{R} and 4 \mathbb{R} BL NLMS filters were selected as $\alpha_{h_i} = \alpha_{g_i} = 0.17$, $\delta_{h_i} = \delta_{g_i} = \delta_{h_{\text{Re}}} = \delta_{h_{\text{Im}}} = \delta_{g_{\text{Re}}} = \delta_{g_{\text{Im}}} = \delta_h$, and $\alpha_{h_{\text{Re}}} = \alpha_{h_{\text{Im}}} = \alpha_{g_{\text{Re}}} = \alpha_{g_{\text{Im}}} = 0.15$, for $i = 1, \dots, 4$. As expected, the CV BL RLS filter is the fastest in convergence, as can be seen in Figure 10. Nevertheless, also the fully CV BL NLMS filter reaches around the same steady state performance. Further, since the unknown BL system can't be appropriately modeled with the 2 \mathbb{R} as well as the 4 \mathbb{R} method, those filters fail to identify the system reasonably.

B. Identification of a Hammerstein system

The following simulation presents the identification of a Hammerstein system, as illustrated in Figure 11.

1) *CV BL NLMS versus CV BL RLS versus 2 \mathbb{R} NLMS versus 4 \mathbb{R} NLMS*: In this section, the goal is to identify a communication transmitter cascaded with a linear channel. Considering the CV baseband, this combination can be modeled as a CV Hammerstein system shown in Figure 11. In this simplified example the communication channel is modeled as a CV finite impulse response (FIR) filter $\mathbf{h} \in \mathbb{C}^L$. I/Q imbalance is introduced as

$$u_k = g_1 x_k + g_2 x_k^* \quad (166)$$

with $g_1 = \frac{1+g_{\text{T}}e^{-j\phi_{\text{T}}}}{2} \in \mathbb{C}$ and $g_2 = \frac{1-g_{\text{T}}e^{j\phi_{\text{T}}}}{2} \in \mathbb{C}$ [41], [42], where a linear power amplifier (PA) is assumed. The amplitude imbalance factor is denoted by $g_{\text{T}} \in \mathbb{R}$, whereas $\phi_{\text{T}} \in \mathbb{R}$ represents the phase imbalance. Now, this signal is convolved with the impulse response of the channel, which produces the output signal

$$y_k = \mathbf{h}^H \begin{bmatrix} x_k & x_k^* \\ \vdots & \vdots \\ x_{k-L+1} & x_{k-L+1}^* \end{bmatrix} \begin{bmatrix} g_1 \\ g_2 \end{bmatrix} = \mathbf{h}^H \mathbf{X}_k \mathbf{g}. \quad (167)$$

From (167) it can be seen, that fully CV BL filters are suitable structures for identifying such a system. On the other hand, because in general (167) cannot be represented with a 2 \mathbb{R} BL filter or a 4 \mathbb{R} BL filter, the identification with a 2 \mathbb{R} BL filter or a 4 \mathbb{R} BL filter is expected to perform worse. The channel impulse response \mathbf{h} with the length $L = 64$ shall model a multipath

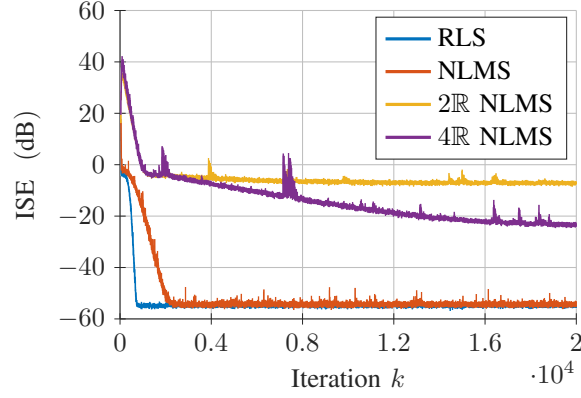


Fig. 12. Convergence behavior of the CV BL RLS filter, the CV BL NLMS filter, the 2R NLMS filter, and the 4R NLMS filter, when identifying a Hammerstein system.

propagation environment and has been chosen similar as in [43]. The amplitude imbalance and the phase imbalance were set to $g_T = 1.15$ and $\phi_T = \frac{\pi}{18}$, respectively. For the fully CV BL NLMS filter, $\alpha_g = \alpha_h = 0.6$ and $\delta_g = \delta_h = 10^{-4}$, were chosen. Further, for the 4R BL NLMS filter the parameters were set to $\alpha_{h_i} = \alpha_{g_i} = 0.012$ and $\delta_{h_i} = \delta_{g_i} = \delta_h$, for $i = 1, \dots, 4$. For the 2R BL NLMS filter $\alpha_{g_{Re}} = \alpha_{g_{Im}} = \alpha_{h_{Re}} = \alpha_{h_{Im}} = 0.01$ and $\delta_{g_{Re}} = \delta_{g_{Im}} = \delta_{h_{Re}} = \delta_{h_{Im}} = \delta_h$ were chosen. Finally, the parameters for the CV BL RLS filter were set to $\lambda = 0.95$, $\mathbf{P}_{h,0} = 10\mathbf{I}^{M \times M}$, and $\mathbf{P}_{g,0} = 10\mathbf{I}^{L \times L}$. The parameters of the CV BL NLMS filter were chosen such that it achieves approximately the same steady state performance as the fully CV BL RLS filter. The parameters for 2R BL filter and the 4R BL filter were chosen to achieve a similar speed of convergence. For the input as well as for the noise signal, complex noise with $x_k \sim \mathcal{CU}(0, 1)$ and $n_k \sim \mathcal{CU}(0, 0.001^2)$, respectively, were chosen. The ISE-performance results of this simulation can be seen in Figure 12. It is evident that using a 2R BL filter or a 4R BL filter results in a high ISE. The other two filters achieve a significantly better and about the same steady state performance. As expected the CV BL RLS filter is the fastest.

V. CONCLUSION

In this work, we introduced several novel CV BL filters for the application to model and identify CV BL systems. First, CV 2R and 4R BL filters were discussed. Next, several fully CV BL filters, including the CV BL WF, the CV BL LS filter, the CV BL LMS filter, the CV BL NLMS filter, and the CV BL RLS filter were introduced. In addition, the update equations for mixed CV-RV BL filters were presented. Furthermore, for the WFs and the LMS-based filters, investigations on the convergence behavior were conducted. Those filters were used to identify MISO systems and Hammerstein models.

APPENDIX

A. Derivation of the mixed CV-RV BL NLMS filter

In this section, one possible method of how to normalize the step-size of the mixed CV-RV BL LMS filter is shown. Similar as in Section III-F for the CV BL NLMS filter, the a-posteriori errors

$$\bar{e}_k = y_k - \hat{\mathbf{h}}_k^H \mathbf{X}_k \hat{\mathbf{g}}_{k-1} \quad (168)$$

and

$$\tilde{e}_k = y_k - \hat{\mathbf{h}}_{k-1}^H \mathbf{X}_k \hat{\mathbf{g}}_k \quad (169)$$

are introduced. Inserting (152) in (168) yields

$$\bar{e}_k = e_k (1 - \mu_h \hat{\mathbf{g}}_{k-1}^H \mathbf{X}_k^H \mathbf{X}_k \hat{\mathbf{g}}_{k-1}). \quad (170)$$

Setting this error to zero and assuming $e_k \neq 0$ we obtain

$$\mu_h = \frac{1}{\hat{\mathbf{g}}_{k-1}^H \mathbf{X}_k^H \mathbf{X}_k \hat{\mathbf{g}}_{k-1}}. \quad (171)$$

Using similar arguments as in Section III-F, the final update equation for $\hat{\mathbf{h}}_k$ follows as

$$\hat{\mathbf{h}}_k = \hat{\mathbf{h}}_{k-1} + \frac{\alpha_h \mathbf{X}_k \hat{\mathbf{g}}_{k-1}}{\delta_h + \hat{\mathbf{g}}_{k-1}^T \mathbf{X}_k^H \mathbf{X}_k \hat{\mathbf{g}}_{k-1}} e_k^*. \quad (172)$$

Since the a-posteriori error in (169) is in general a CV number, it might not be possible to set it to zero using a RV update for $\hat{\mathbf{g}}_k$. Setting (169) to zero would require a CV step-size $\mu_{\mathbf{g}}$. A meaningful step-size is the one that minimizes $|\tilde{e}_k|^2$. With (169)

$$|\tilde{e}_k|^2 = y_k y_k^* - 2 \operatorname{Re} \left[y_k^* \hat{\mathbf{h}}_{k-1}^H \mathbf{X}_k \right] \hat{\mathbf{g}}_k + \hat{\mathbf{g}}_k^T \mathbf{X}_k \hat{\mathbf{h}}_{k-1} \hat{\mathbf{h}}_{k-1}^H \mathbf{X}_k \hat{\mathbf{g}}_k. \quad (173)$$

After inserting (153) the gradient follows to

$$\frac{\partial |\tilde{e}_k|^2}{\partial \mu_{\mathbf{g}}} = -2 \operatorname{Re} \left[e_k^* \hat{\mathbf{h}}_{k-1}^H \mathbf{X}_k \right] \operatorname{Re} \left[e_k \mathbf{X}_k^H \hat{\mathbf{h}}_{k-1} \right] + 2 \mu_{\mathbf{g}} \operatorname{Re} \left[e_k \hat{\mathbf{h}}_{k-1}^T \mathbf{X}_k^* \right] \mathbf{X}_k^H \hat{\mathbf{h}}_{k-1} \hat{\mathbf{h}}_{k-1}^H \mathbf{X}_k \operatorname{Re} \left[e_k \mathbf{X}_k^H \hat{\mathbf{h}}_{k-1} \right]. \quad (174)$$

Setting this to zero yields the optimal step-size

$$\mu_{\mathbf{g}} = \operatorname{Re} \left[e_k^* \hat{\mathbf{h}}_{k-1}^H \mathbf{X}_k \right] \frac{\operatorname{Re} \left[e_k \mathbf{X}_k^H \hat{\mathbf{h}}_{k-1} \right]}{\operatorname{Re} \left[e_k \hat{\mathbf{h}}_{k-1}^T \mathbf{X}_k^* \right] \mathbf{X}_k^H \hat{\mathbf{h}}_{k-1} \hat{\mathbf{h}}_{k-1}^H \mathbf{X}_k \operatorname{Re} \left[e_k \mathbf{X}_k^H \hat{\mathbf{h}}_{k-1} \right]}. \quad (175)$$

Again similar as in Section III-F, the second update equation results in

$$\hat{\mathbf{g}}_k = \hat{\mathbf{g}}_{k-1} + \alpha_{\mathbf{g}} 2 \operatorname{Re} \left[e_k \mathbf{X}_k^H \hat{\mathbf{h}}_{k-1} \right] \frac{\operatorname{Re} \left[e_k^* \hat{\mathbf{h}}_{k-1}^H \mathbf{X}_k \right] \operatorname{Re} \left[e_k \mathbf{X}_k^H \hat{\mathbf{h}}_{k-1} \right]}{\delta_{\mathbf{g}} + \operatorname{Re} \left[e_k \hat{\mathbf{h}}_{k-1}^T \mathbf{X}_k^* \right] \mathbf{X}_k^H \hat{\mathbf{h}}_{k-1} \hat{\mathbf{h}}_{k-1}^H \mathbf{X}_k \operatorname{Re} \left[e_k \mathbf{X}_k^H \hat{\mathbf{h}}_{k-1} \right]}. \quad (176)$$

REFERENCES

- [1] S. M. Kay, *Fundamentals of Statistical Signal Processing: Estimation Theory*. Prentice Hall, 1993.
- [2] P. Diniz, *Adaptive Filtering: Algorithms and Practical Implementation*. Springer Cham, 2008.
- [3] A. Tülay and S. Haykin, *Adaptive Signal Processing: Next Generation Solutions*. John Wiley and Sons, 2010.
- [4] V. Volterra, *Theory of Functionals and of Integral and Integro-Differential Equations*. Cambridge University Press, 1959.
- [5] S. Haykin, *Neural Networks and Learning Machines*. Prentice Hall, 1999.
- [6] M. Scarpiniti, D. Communiello, R. Parisi, and A. Uncini, "Nonlinear spline adaptive filtering," *IEEE Signal Process. Mag.*, vol. 93, no. 4, pp. 772–783, 2013.
- [7] P. L. dos Santos, J. A. Ramos, and J. de Carvalho, "Identification of Bilinear Systems With White Noise Inputs: An Iterative Deterministic-Stochastic Subspace Approach," *IEEE Trans. on Control Systems Technol.*, vol. 17, no. 5, pp. 1145–1153, 2009.
- [8] U. Forssen, "Adaptive bilinear digital filters," *IEEE Trans. on Circuits and Systems II: Analog and Digital Signal Process.*, vol. 40, no. 11, pp. 729–735, 1993.
- [9] R. Hu and H. M. Ahmed, "Echo cancellation in high speed data transmission systems using adaptive layered bilinear filters," *IEEE Trans. on Commun.*, vol. 42, no. 2/3/4, pp. 655–663, 1994.
- [10] S. M. Kuo and H.-T. Wu, "Nonlinear adaptive bilinear filters for active noise control systems," *IEEE Trans. on Circuits and Systems I: Regular Papers*, vol. 52, no. 3, pp. 617–624, 2005.
- [11] G.-K. Ma, J. Lee, and V. J. Mathews, "A RLS bilinear filter for channel equalization," in Proc. IEEE ICASSP, pp. III/257–III/260, 1994.
- [12] Z. Zhu and H. Leung, "Adaptive identification of nonlinear systems with application to chaotic communications," *IEEE Trans. on Circuits and Systems I: Fundamental Theory and Applications*, vol. 47, no. 7, pp. 1072–1080, 2000.
- [13] J. Benesty, C. Paleologu, and S. Ciochina, "On the Identification of Bilinear Forms With the Wiener Filter," *IEEE Signal Process. Lett.*, vol. 24, no. 5, pp. 653–657, 2017.
- [14] E.-W. Bai and Y. Liu, "Least squares solutions of bilinear equations," *Systems and Control Letters*, vol. 55, no. 6, pp. 466–472, 2006.
- [15] S. Ciochina, C. Paleologu, and J. Benesty, "Analysis of an LMS algorithm for bilinear forms," in Proc. Int. Conf. on Digital Signal Process. (DSP), pp. 1–5, 2017.
- [16] L.-M. Dogariu, S. Ciochina, C. Paleologu, J. Benesty, and P. Piantanida, "An Optimized LMS Algorithm for Bilinear Forms," in Proc. Int. Symp. on Electronics and Telecommun. (ISETC), pp. 1–5, 2018.
- [17] C. Paleologu, J. Benesty, and S. Ciochina, "An NLMS algorithm for the identification of bilinear forms," in Proc. Eur. Signal Process. Conf. (EUSIPCO), pp. 2620–2624, 2017.
- [18] C. Elisei-Iliescu, C. Paleologu, R. A. Dobre, S. Ciochina, and J. Benesty, "An RLS algorithm for the identification of bilinear forms," in Proc. IEEE Int. Symp. for Design and Technol. in Electronic Packaging (SIITME), pp. 292–295, 2017.
- [19] C. Elisei-Iliescu, C. Paleologu, C. Stanciu, C. Anghel, S. Ciochina, and J. Benesty, "Regularized Recursive Least-Squares Algorithms for the Identification of Bilinear Forms," in Proc. Int. Symp. on Electronics and Telecommun. (ISETC), 2018.
- [20] C. Elisei-Iliescu, C. Stanciu, C. Paleologu, J. Benesty, C. Anghel, and S. Ciochina, "Efficient recursive least-squares algorithms for the identification of bilinear forms," *Digital Signal Process.*, vol. 83, pp. 280–296, 2018.
- [21] C. Elisei-Iliescu, C. Stanciu, C. Paleologu, C. Anghel, S. Ciochina, and J. Benesty, "Low-Complexity RLS Algorithms for the Identification of Bilinear Forms," in Proc. Eur. Signal Process. Conf. (EUSIPCO), pp. 455–459, 2018.
- [22] L.-M. Dogariu, C. Paleologu, S. Ciochina, J. Benesty, and P. Piantanida, "Identification of Bilinear Forms with the Kalman Filter," in Proc. IEEE Int. Conf. on Acoustics, Speech and Signal Process. (ICASSP), pp. 4134–4138, 2018.
- [23] C. Paleologu, J. Benesty, and S. Ciochina, "Adaptive filtering for the identification of bilinear forms," *Digital Signal Process.*, vol. 75, pp. 153–167, 2018.
- [24] J. Benesty, C. Paleologu, L.-M. Dogariu, and S. Ciochina, "Identification of Linear and Bilinear Systems: A Unified Study," *Electronics*, vol. 10, no. 15, 2021.
- [25] M. Wagner, O. Lang, E. K. Ghafi, A. Preniqi, A. Schwarz, and M. Huemer, "Bi-Linear Homogeneity Enforced Calibration for Pipelined ADCs," 2025.
- [26] D. Gesbert and P. Duhamel, "Robust blind joint data/channel estimation based on bilinear optimization," in *Proceedings of 8th Workshop on Statistical Signal and Array Processing*, pp. 168–171, 1996.
- [27] G. Qian, D. Luo, and S. Wang, "A Robust Adaptive Filter for a Complex Hammerstein System," *Entropy (Basel, Switzerland)*, vol. 21, no. 2, 2019.
- [28] P. P. Campo, D. Korpi, L. Anttila, and M. Valkama, "Nonlinear Digital Cancellation in Full-Duplex Devices using Spline-Based Hammerstein Model," in *IEEE Globecom Workshops (GC Wkshps)*, 2018.
- [29] P. Pascual Campo, L. Anttila, D. Korpi, and M. Valkama, "Cascaded Spline-Based Models for Complex Nonlinear Systems: Methods and Applications," *IEEE Trans. on Signal Process.*, vol. 69, pp. 370–384, 2021.

- [30] T. Paireder, C. Motz, and M. Huemer, "Spline-Based Adaptive Cancellation of Even-Order Intermodulation Distortions in LTE-A/5G RF Transceivers," *IEEE Trans. on Veh. Technol.*, vol. 70, no. 6, pp. 5817–5832, 2021.
- [31] T. Adali, P. J. Schreier, and L. L. Scharf, "Complex-valued signal processing: The proper way to deal with impropriety," *IEEE Trans. on Signal Process.*, vol. 59, no. 11, pp. 5101–5125, 2011.
- [32] D. Mandic and V. Su Lee Goh, *Complex Valued Nonlinear Adaptive Filter*. John Wiley and Sons, 2009.
- [33] M. Scarpiniti, D. Communiello, R. Parisi, and A. Uncini, "Spline Adaptive Filters," in *Adaptive Learning Methods for Nonlinear System Modeling*. Elsevier, 2018.
- [34] C. Liu and H. Zhao, "A 2D-LUT Scheme Design for Complex-Valued Spline Adaptive Filter," *IEEE Trans. on Circuits and Systems II: Express Briefs*, vol. 70, no. 8, pp. 3154–3158, 2023.
- [35] P. J. Schreier and L. L. Scharf, "Statistical Signal Processing of Complex-Valued Data: The Theory of Improper and Noncircular Signals." Cambridge University Press, 2010.
- [36] O. Lang, "Knowledge-Aided Methods in Estimation Theory and Adaptive Filtering," PhD thesis conducted at the Johannes Kepler University Linz, Austria, 2018.
- [37] W. Wirtinger, "Zur formalen Theorie der Funktionen von mehr komplexen Veränderlichen," *Mathematische Annalen*, vol. 97, pp. 357–375.
- [38] L. Malathi, A. Bharathi, and A. Jayanthi, "Review On Fast Complex Multiplication Algorithms and Implementation," *Int. Journal of Current Engineering and Scientific Research*, 2019.
- [39] A. Gebhard, O. Lang, M. Lunglmayr, C. Motz, R. S. Kanumalli, C. Auer, T. Paireder, M. Wagner, H. Pretl, and M. Huemer, "A Robust Nonlinear RLS Type Adaptive Filter for Second-Order-Intermodulation Distortion Cancellation in FDD LTE and 5G Direct Conversion Transceivers," *IEEE Transactions on Microwave Theory and Techniques*, vol. 67, no. 5, pp. 1946–1961, 2019.
- [40] M. Woodbury and P. U. D. of Statistics, *Inverting Modified Matrices*, ser. Memorandum Report / Statistical Research Group, Princeton. Department of Statistics, Princeton University, 1950.
- [41] M. Valkama, M. Renfors, and V. Koivunen, "Advanced methods for I/Q imbalance compensation in communication receivers," *IEEE Trans. on Signal Process.*, vol. 49, no. 10, pp. 2335–2344, 2001.
- [42] M. Tockner, M. Stockinger, O. Lang, A. Meingassner, and M. Huemer, "Extensive Comparison of Blind I/Q Imbalance Estimator Hardware Requirements," in *2024 Austrochip Workshop on Microelectronics (Austrochip)*, pp. 1–4, 2024.
- [43] C. Hofbauer, "Design and analysis of unique word OFDM," PhD thesis conducted at the University Klagenfurt, Austria, 2016.